ปฏิกิริยาดีไฮเดรชันของเอทานอลบนตัวเร่งปฏิกิริยาเบต้าซีโอไลท์

นางสาวธนัชพร คำสุวรรณ์

วิทยานิพนธ์นี้เป็นส่วนหนึ่งของการศึกษาตามหลักสูตรปริญญาวิศวกรรมศาสตรมหาบัณฑิต
สาขาวิชาวิศวกรรมเคมี ภาควิชาวิศวกรรมเคมี
คณะวิศวกรรมศาสตร์ จุฬาลงกรณ์มหาวิทยาลัย
ปีการศึกษา 2558

DEHYDRATION REACTION OF ETHANOL OVER BETA ZEOLITE CATALYST

Miss Tanutporn Kamsuwan

A Thesis Submitted in Partial Fulfillment of the Requirements

for the Degree of Master of Engineering Program in Chemical Engineering

Department of Chemical Engineering

Faculty of Engineering

Chulalongkorn University

Academic Year 2015

Thesis Title	DEHYDRATION REACTION OF ETHANOL OVER BETA ZEOLITE CATALYST
By	Miss Tanutporn Kamsuwan
Field of Study	Chemical Engineering
Thesis Advisor	Associate Professor Bunjerd Jongsomjit, Ph.D.

Accepted by the Faculty of Engineering, Chulalongkorn University in Partial Fulfillment of the Requirements for the Master's Degree

.....Dean of the Faculty of Engineering

(Professor Bundhit Eua-arporn, Ph.D.)

THESIS COMMITTEE

.....Chairman

(Associate Professor Muenduen Phisalaphong, Ph.D.)

.....Thesis Advisor

(Associate Professor Bunjerd Jongsomjit, Ph.D.)

.....Examiner

(Chutimon Satirapipathkul, D.Eng.)

.....External Examiner

(Ekrachan Chaichana, D.Eng.)

ธนัชพร คำสุวรรณ์ : ปฏิกิริยาดีไฮเดรชันของเอทานอลบนตัวเร่งปฏิกิริยาเบต้าซีโอไลท์ (DEHYDRATION REACTION OF ETHANOL OVER BETA ZEOLITE CATALYST) อ.ที่ปรึกษาวิทยานิพนธ์หลัก: รศ. ดร.บรรเจิด จงสมจิตร, 90 หน้า.

ตัวเร่งปฏิกิริยาที่มีความแตกต่างกันของโครงสร้างอลูมินา 3 ชนิด ประกอบด้วย เบต้าซีโอไลท์ การดัดแปลงเบต้าซีโอไลท์ด้วยแกมมาอลูมินา และวัฏภาคผสมแกมมา และไคของอะลูมินา ถูกนำมาศึกษาคุณสมบัติและประสิทธิภาพของตัวเร่งปฏิกิริยาผ่านปฏิกิริยาการขจัดน้ำของเอทานอล นอกจากนี้ยังศึกษาการผลิตไดเอทิลอีเทอร์และการปรับปรุงความสามารถของตัวเร่งปฏิกิริยาในปฏิกิริยาการขจัดน้ำของเอทานอล โดยศึกษาตัวเร่งปฏิกิริยาที่มีการดัดแปลงของเบต้าซีโอไลท์ด้วยรูเทเนียมและแพลตทินัมเปรียบเทียบกับเบต้าซีโอไลท์ที่ไม่ถูกดัดแปลง ตัวเร่งปฏิกิริยาถูกวิเคราะห์คุณลักษณะด้วยการกระเจิงรังสีเอ็กซ์ การดูดซับทางกายภาพด้วยไนโตเจน กล้องจุลทรรศน์อิเล็กตรอนแบบส่องกราด การคายแอมโมเนียด้วยการเพิ่มอุณหภูมิแบบตั้งโปรแกรม และการวิเคราะห์การสลายตัวของสารเมื่อได้รับความร้อน ความสามารถของตัวเร่งปฏิกิริยาในปฏิกิริยาการขจัดน้ำของเอทานอลในวัฏภาคแก๊สถูกทดสอบที่ความดันบรรยากาศ และอุณหภูมิระหว่าง 200 ถึง 400 องศาเซลเซียส ในขณะที่การศึกษาประสิทธิภาพของตัวเร่งปฏิกิริยาถูกทดสอบผ่านเวลาที่ใช้ในการดำเนินการปฏิกิริยาที่ 10 และ 72 ชั่วโมงตามอุณหภูมิที่เหมาะสม จากการศึกษาพบว่าเบต้าซีโอไลท์ให้ร้อยละการเกิดผลิตภัณฑ์และความสามารถของตัวเร่งปฏิกิริยาสูงที่สุด เนื่องจากเบต้าซีโอไลท์มีพื้นที่ผิวและปริมาณของตำแหน่งความเป็นกรดอ่อนในปริมาณสูงมากที่ทำให้เกิดผลิตภัณฑ์ในปฏิกิริยา การดัดแปลงเบต้าซีโอไลท์ด้วยรูเทเนียมและแพลตทินัมที่ทำหน้าที่เป็นตัวส่งเสริมให้เกิดการเกิดปฏิกิริยานั้น สามารถเพิ่มพื้นที่ผิวของตัวเร่งปฏิกิริยาสำหรับโอกาสในการเพิ่มความสามารถของตัวเร่งปฏิกิริยาในปฏิกิริยาการขจัดน้ำของเอทานอลเพื่อผลิตไดเอทิลอีเทอร์ การเพิ่มของรูเทเนียมบนเบต้าซีโอไลท์นั้นถือเป็นข้อดีสำหรับเพิ่มร้อยละผลผลิตของไดเอทิลอีเทอร์ที่อุณหภูมิการเกิดปฏิกิริยาที่ 250 องศาเซลเซียสสำหรับสภาวะการเกิดปฏิกิริยานี้ ร้อยละผลผลิตของไดเอทิลอีเทอร์ที่มากที่สุด (35%) นั้นได้รับจากการดัดแปลงตัวเร่งปฏิกิริยาเบต้าซีโอไลท์ด้วยรูเทเนียมที่อุณหภูมิการเกิดปฏิกิริยาที่ 250 องศาเซลเซียส

ภาควิชา วิศวกรรมเคมี ลายมือชื่อนิสิต .....

สาขาวิชา วิศวกรรมเคมี ลายมือชื่อ อ.ที่ปรึกษาหลัก .....

ปีการศึกษา 2558

5770192321 : MAJOR CHEMICAL ENGINEERING

KEYWORDS: ETHYLENE; DIETHYL ETHER; ETHANOL DEHYDRATION; AL-BASED CATALYSTS; ZEOLITE;NOBLE METAL

TANUTPORN KAMSUWAN: DEHYDRATION REACTION OF ETHANOL OVER BETA ZEOLITE CATALYST. ADVISOR: ASSOC. PROF. BUNJERD JONGSOMJIT, Ph.D., 90 pp.

Three different Al-based solid acid catalysts including H-beta zeolite (HBZ), modified H-beta zeolite with γ-Al_2O_3 (Al-HBZ) and mixed γ- χ phase of Al_2O_3 (M-Al) catalysts were investigated for catalytic properties and performance via ethanol dehydration. In addition, DEE production via ethanol dehydration and improvement of catalytic activity were also studied over Ru and Pt modification of H-beta zeolite catalysts demoted as Ru- and Pt- modified H-beta zeolite (Ru-HBZ and Pt-HBZ) catalysts. The catalysts were characterized by X-ray diffraction (XRD), N_2 physisorption, scanning electron microscopy (SEM), energy dispersive X-ray spectroscopy (EDX), NH_3-tempearture programmed desorption (NH_3-TPD) and thermal gravimetric analysis (TGA). The catalytic activity was tested for ethylene production by dehydration reaction of ethanol in gas phase at atmospheric pressure and temperature between 200 to 400°C. Meanwhile, the time-on-stream of the catalyst for 10 and 72 h during the reaction at suitable temperature was determined for catalytic performance. It was found that the HBZ catalyst exhibited the highest products yield and catalytic activity because it has the highest surface area and amount of weak acid site for catalyzing this reaction. In addition, the modification of HBZ with Ru- and Pt- as promoters could enhance the surface area for opportunity in increasing catalytic activity, which is suitable for ethanol dehydration to DEE. The addition of Ru over HBZ is advantage to increase the DEE yield at 250°C for this condition. The maximum yield of DEE (35%) was obtained from Ru-HBZ at 250°C.

Department: Chemical Engineering Student's Signature .....

Field of Study: Chemical Engineering Advisor's Signature .....

Academic Year: 2015

ACKNOWLEDGEMENTS

I would like to impressively thank my thesis advisor, Associate Professor Bunjerd Jongsomjit, Ph.D. for his advice and guidance in order to solve the problem in this research as well as invaluable help, understanding and continued support. I realize the teachings of his. This thesis cannot be achieved without my advisor.

Furthermore, I also have to thank Associate Professor Muenduen Phisalaphong, Ph.D, as a chairman, Dr. Chutimon Satirapipathkul, D.Eng and Dr. Eakrachan Chaichana, D.Eng as the members of the thesis committee for suggestions and taking valuable time to review this thesis.

The authors thank the Thailand Research Fund (TRF), the National Research Council of Thailand (NRCT) and Ratchadaphiseksomphot Endowment Fund (2015) of Chulalongkorn University (CU-58-027- AM) for financial support of this project.

Finally, I most gratefully acknowledge my parents, Dr. Mingkwan Wannaborworn, co-worker and my friends in Center of Excellence on Catalysis and Catalytic Reaction Engineering laboratory for all support and carefulness.

CONTENTS

Page

Page

Page

LIST OF TABLES

LIST OF FIGURES

CHAPTER I
INTRODUCTION

1.1 General introduction

Ethylene is an essential material in the petroleum industry. It is produced from crude oil and the most normally used as feedstocks to produce ethylene oxide (EO) and variety of polymers in petrochemical industry such as polyethylene (PE), polyethylene terephthalate (PET), polyvinyl chloride (PVC), and polystyrene (PS) [1-3]. Currently, ethylene is mainly obtained by thermal catalytic cracking of higher hydrocarbons, such as naphtha. This process is highly energy intensive, low production cost and CO_2 emissions worldwide. This reaction is an endothermic reaction, which is required high temperatures about 600 to 1000°C [2, 4, 5]. Therefore, the new suitable way to produce ethylene instead of thermal catalytic cracking is considered for development to enhance ethylene production. So, the dehydration of ethanol has been considered as promising alternative route approach to produce ethylene. Ethanol can be converted into ethylene by catalytic dehydration, which must occur over acid catalysts. Dehydration of ethanol over solid acid catalysts requires lower temperature when compared with the thermal cracking, leading to the reduction of energy cost and increasing of productivity. The main product from this reaction is ethylene, whereas diethyl ether (DEE), acetaldehyde and light olefins are byproducts. Each of products is produced at the different temperatures. Furthermore, yield and productivity depend on nature of acid catalyst types used. Acid catalytic dehydration of ethanol to ethylene was investigated using the supported phosphoric acid, alumina, zeolite, silica–alumina and transition metal oxide (such as titanium oxides, magnesium oxides, cobalt oxides, chromium oxide and silver salt of tungstophosphoric acid) [5-9].

In general, HZSM-5 zeolite as solid acid catalyst is mostly used for the ethanol dehydration into ethylene due to the temperature of this reaction over HZSM-5 zeolite catalyst was lower than other catalysts. In addition, HZSM-5 zeolite catalyst exhibits the highly activity and selectivity of ethylene, but it has low stability. Because of the high acidity of HZSM-5 zeolite, it is the disadvantage for dehydration. It leads to the

coke formation on its surface, which results in catalyst deactivation (decreases of activity and selectivity to ethylene) [10, 11]. Thus, alumina (Al_2O_3), silica-alumina and modified zeolite (alumino-silicate materials) were used as catalysts for ethanol dehydration, which is alternative way for improvement of the catalytic performance [12]. Each type of solid catalyst has a different structure and properties such as the physicochemical properties of alumina catalysts depending on the methods of preparation and calcination conditions. It is known that there are many methods to synthesize alumina catalysts such as solvothermal synthesis, sol-gel synthesis, flame spray hydrolysis, precipitation, emulsion evaporation, microwave synthesis, hydrothermal synthesis and heat treatment of aluminium hydroxides [13, 14]. The solvothermal and sol-gel methods are commonly used for synthesis of alumina. The γ-Al_2O_3 and mixed phase γ-χ-Al_2O_3 catalysts were also investigated for this reaction because they exhibit high thermal stability, fine particle size, high surface area, large pore volume, inhibit side reaction and high acidity, which is enough to produce ethylene via ethanol dehydration. Janlamool and Jongsomjit [15], Huang et al. [16] and Pansanga et al. [17] studied the synthesis of mixed γ- and χ- phase Al_2O_3 catalysts. They reported that the acidity of mixed γ- and χ- phase Al_2O_3 is higher than γ-Al_2O_3 and χ-Al_2O_3. The mixed γ- and χ- phase Al_2O_3 catalysts can be synthesized directly by using the solvothermal method via suitable solvent in order to control structures, grain sizes and morphologies by varying process conditions [15-17]. Although, there have many reports about using HZSM-5 zeolite as catalyst for ethanol dehydration, but there have been no reports of the ethanol dehydration to ethylene over H-beta zeolite. It is microporous zeolite having high surface area, high thermal stability and high acidity. Moreover, H-beta zeolite exhibits larger pore size than H-ZSM-5 and it is expected to produce hydrocarbon with less coke deposition due to higher diffusivity in the pore [18]. It is interesting for being used as a catalyst for dehydration. Furthermore, the catalyst was modified by adding metal into surface catalyst that can improve catalytic performance and surface properties [5, 8, 18, 19].

In this research, we aimed to develop the alumina-based solid acid catalysts for ethanol dehydration. The catalysts were synthesized, characterized and tested at

a specified reaction condition. The synthesis parameters and reaction conditions influencing on dehydration reaction were varied in order to explore the suitable catalysts and conditions for ethanol dehydration. The catalysts were characterized using various techniques.

1.2 Research objectives

1.) To investigate the characteristics, catalytic properties and catalytic performance of Al-based solid acid catalysts including H-beta zeolite (HBZ), modified H-beta zeolite with γ-Al_2O_3 (Al-HBZ) and mixed γ- χ phase of Al_2O_3 (M-Al) catalysts for ethanol dehydration reaction.

2.) To measure yield and productivity by using modified H-beta zeolite with noble metal to increase catalytic activity at low reaction temperature.

1.3 Research scopes

1.) Using Al-based solid acid catalysts including H-beta zeolite (HBZ), modified H-beta zeolite with γ-Al_2O_3 (Al-HBZ) and mixed γ-χ-phase of Al_2O_3 (M-Al) catalysts over the ethanol dehydration.

2.) Testing product distribution in ethanol dehydration over Al-based solid acid catalysts at 1 atm and 200 to 400°C.

3.) Testing catalytic performance of Al-based solid acid catalysts over the ethanol dehydration at 1 atm and 400°C for 72 h.

4.) Investigate modified H-beta zeolite with noble metal

5.) Testing catalytic activity modified H-beta zeolite with noble metal over the ethanol dehydration at 1 atm for time on stream at low reaction temperature.

6.) Characterization of the catalysts by the following method;

- X-ray diffraction (XRD)
- N_2 physisorption
- Scanning electron microscopy (SEM) and energy dispersive X-ray spectroscopy (EDX)
- Temperature-programmed desorption of ammonia (NH_3-TPD)

- Thermal gravimetric analysis (TGA)

1.4 Research methodology

Research methodology is as shown;

Part I: Comparative study of catalytic activity of Al-based solid acid catalysts.

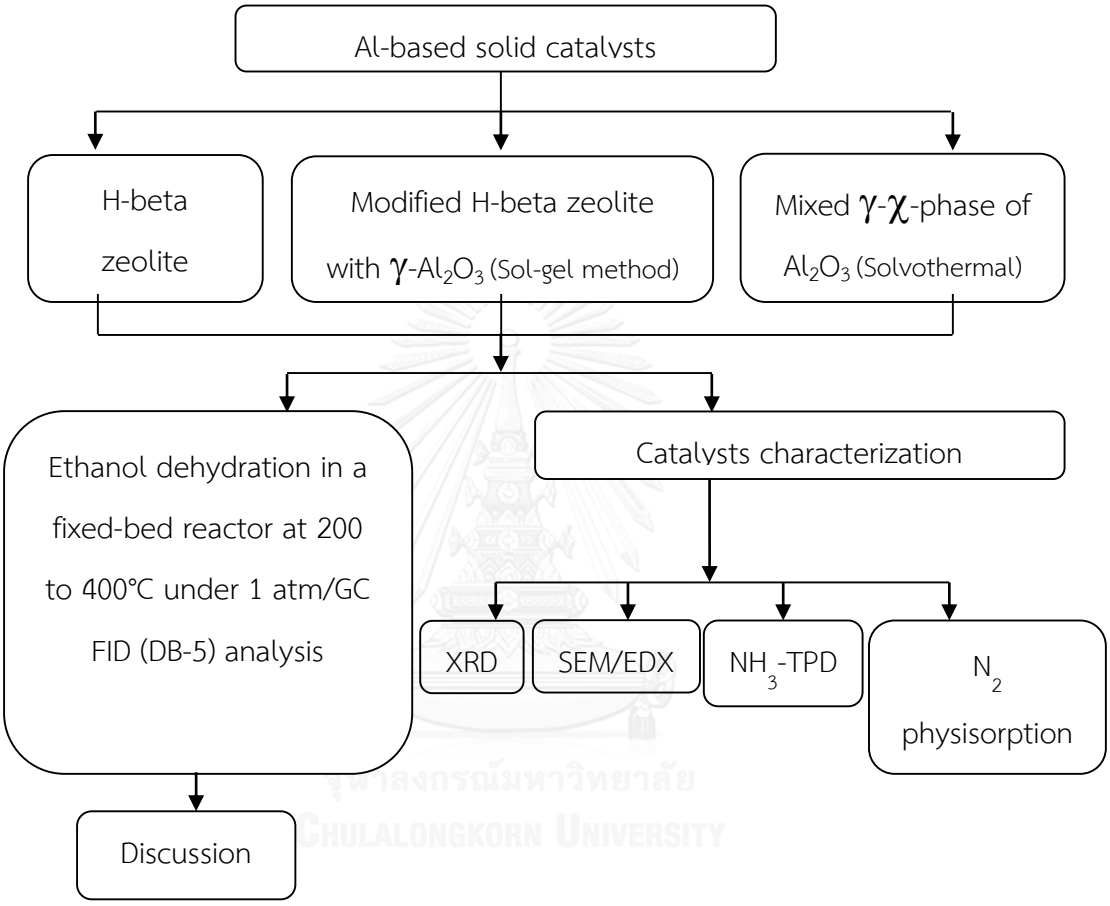

Part II: Investigation of catalytic stability of Al-based solid acid catalysts.

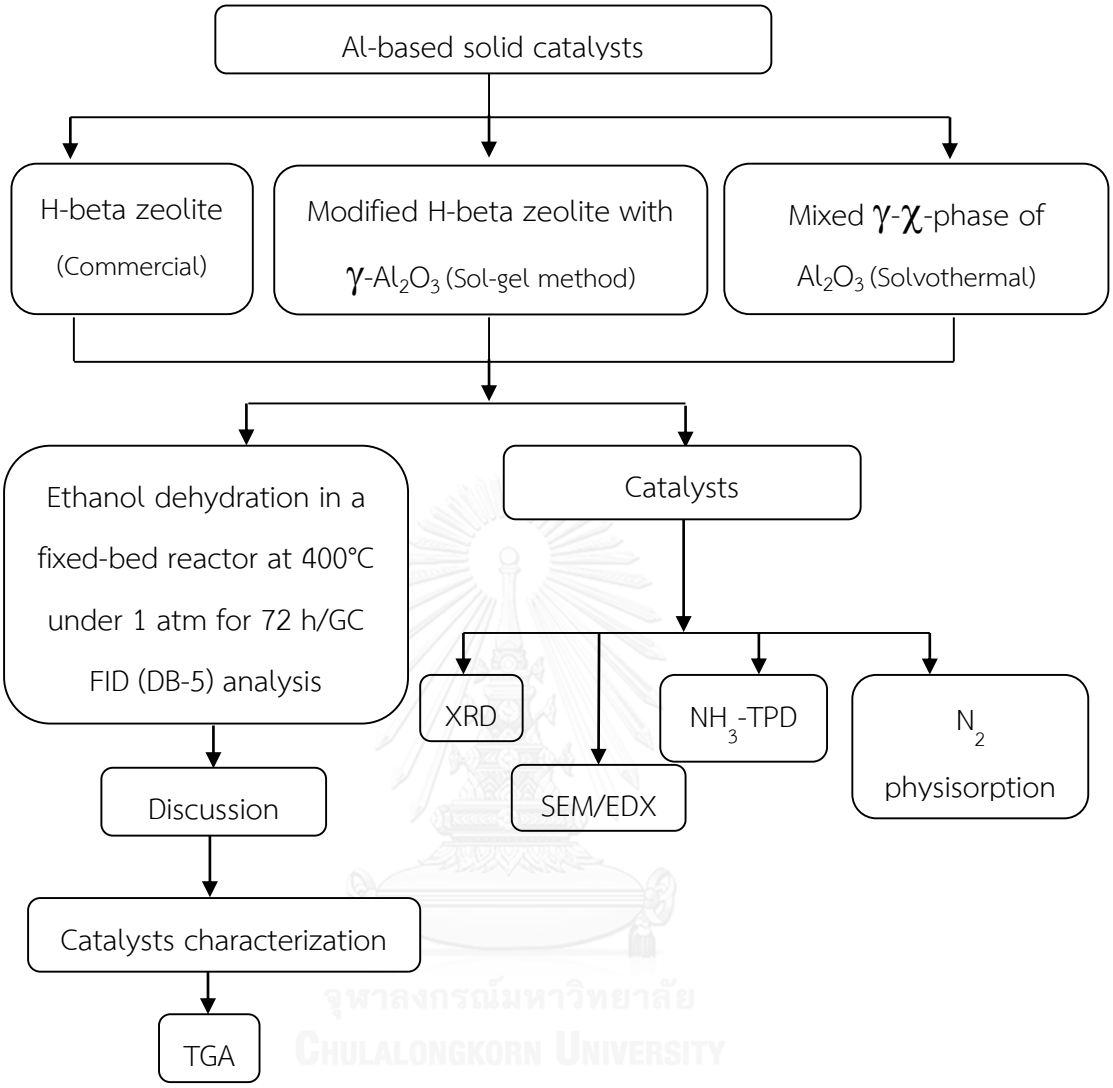

Part III: Investigate modified H-beta zeolite with noble metal

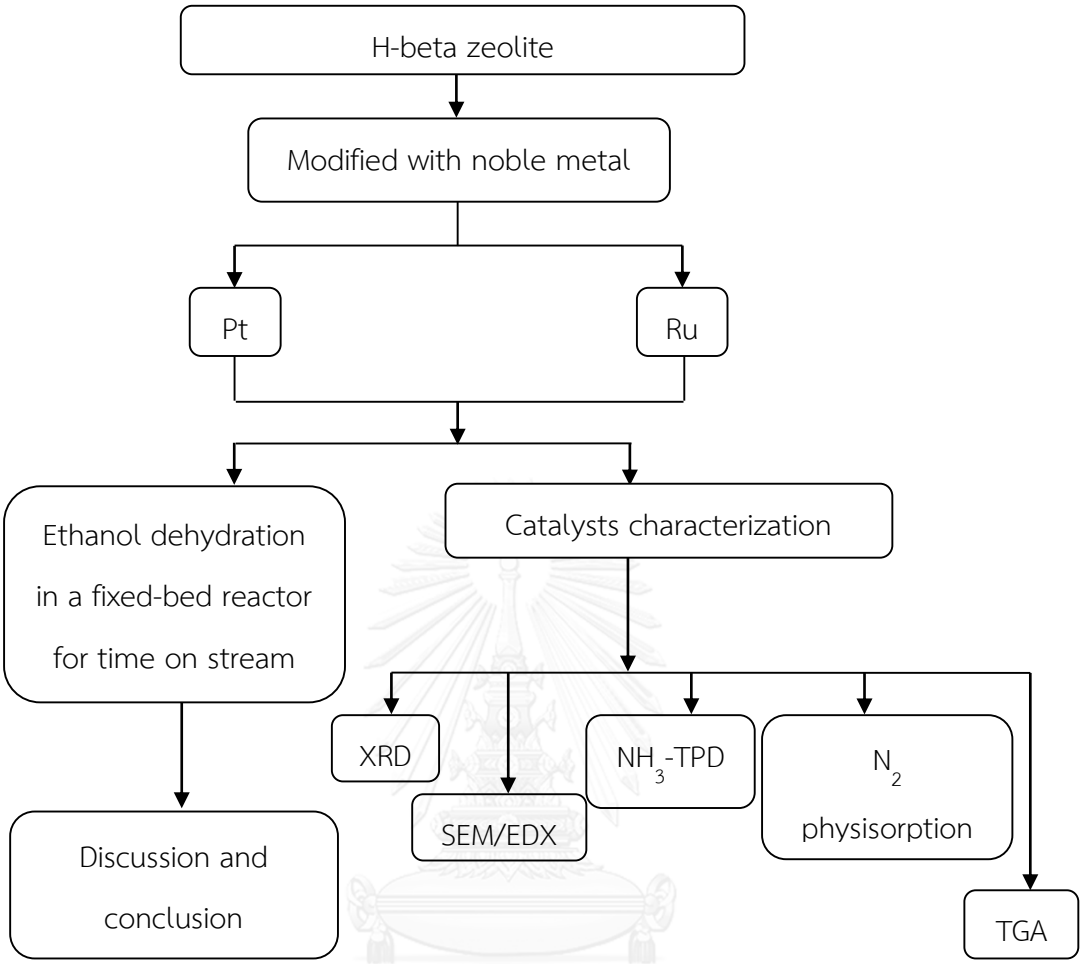

As mentioned above, it explains about the motivation of the research, the research scopes, and the research methodology. Henceforth, the content of thesis is arranged as follows:

Chapter 2 contains basic knowledge of ethanol dehydration reaction and the catalysts used in ethanol dehydration reaction.

Chapter 3 is the literature reviews

Chapter 4 describes the experimental procedure for catalysts preparation, procedures for reaction testing, and instrument for characterization.

CHAPTER II
THEORIES

The benefit of ethanol is well known as a solvent. However, it is able to produce a variety of products such as ethylene, diethyl ether (DEE), acetaldehyde, styrene and etc. Ethylene is produced through dehydration reaction of ethanol by using solid acid catalyst. The basic knowledge of ethanol dehydration reaction and the solid acid catalysts used in this reaction follows in Chapter 2.

2.1 Ethanol dehydration reaction

Ethanol consists of hydroxyl group in molecule. It can be dehydrated by using solid acid catalysts. The hydroxyl group is converted into water molecule. After the water molecule is emitted from ethanol molecule, the hydrocarbon rearranges into ethylene or DEE [20]. In addition to the main product of ethylene and the main byproduct of ether, the reaction of ethanol dehydration may also generate a small amount of byproducts such as acetaldehyde, hydrocarbons (methane, ethane, propylene) and so on [21]. Two competitive ways occur during ethanol dehydration as follows [22];

$C_2H_5OH \longrightarrow C_2H_4 + H_2O$ +44.9 kJ/mol (1)

$2C_2H_5OH \longrightarrow C_2H_5OC_2H_5 + H_2O$ -25.1 kJ/mol (2)

The first reaction (main reaction, intra-molecular dehydration of ethanol to ethylene) is endothermic while the second reaction (side reaction, inter-molecular dehydration of ethanol to diethyl-ether) is exothermic. Diethyl-ether is produced in significant quantities at low temperature; however, ethylene is occurred at high temperature [22]. The mechanism of ethanol dehydration reaction is believed to be the parallel surface reactions or the series reactions. In the parallel surface reactions, ethanol molecules are changed into ethylene molecules together with diethyl ether molecules. While in the series reaction, molecules of ethanol are converted to diethyl ether molecules after that changing to ethylene molecules [21]. The mechanism of reactions is shown in **Figure 2.1**.

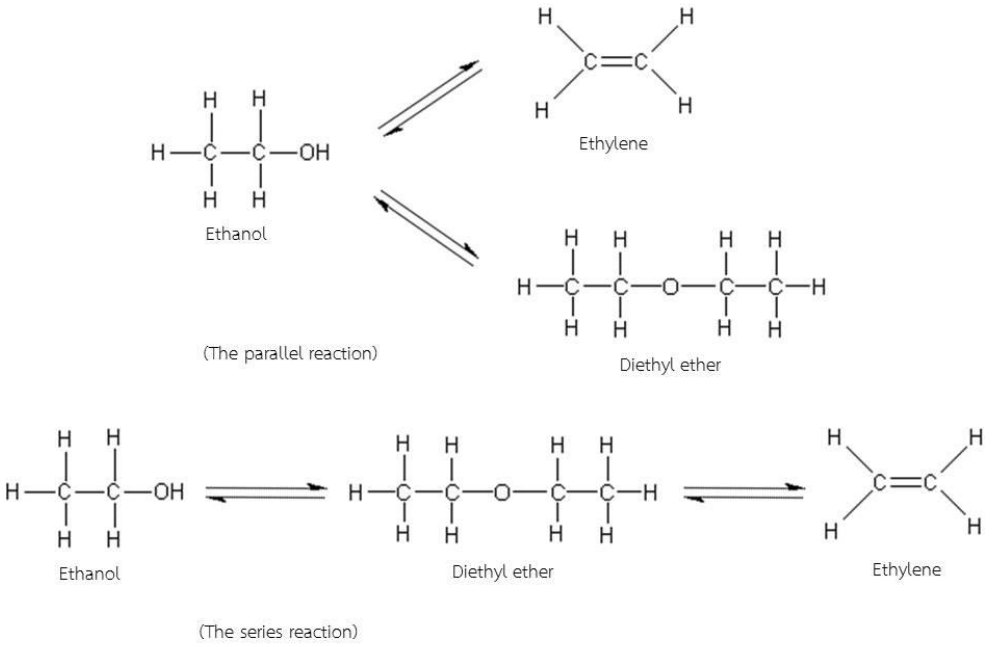

Figure 2.1 Mechanism of dehydration for ethanol dehydration: the parallel reaction and the series reaction [21].

Ethylene is formed by catalytic dehydration of ethanol which requires one ethanol molecule to generate carbocation during the reaction. In the First, the proton from acid catalyst protonates the hydroxyl group of ethanol molecule to remove the water molecule. Then, the conjugate base of the catalyst then deprotonates the methyl group, and the hydrocarbon rearranges into ethylene [3]. This reaction requires strong acid site or Bronsted acid site [9, 23-25] and high operating temperature (in the range of 180 to 500°C) [3]. The mechanism of reaction is shown in **Figure 2.2**.

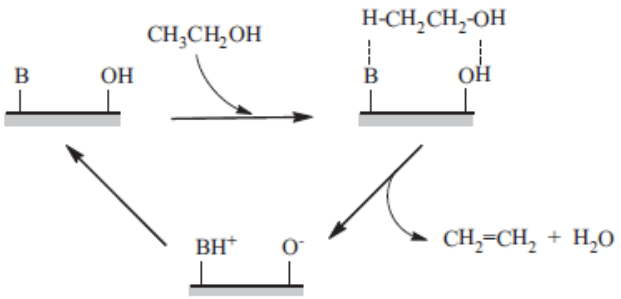

Figure 2.2 Mechanism of ethanol dehydration to ethylene at base (B) and Brønsted acid (OH) catalyst sites [25].

The dehydration of ethanol converts ethanol molecules into diethyl ether. This reaction requires weak acid site and low operating temperature (below 240°C). It known that this reaction requires two ethanol molecules, and no generation of carbocation taking place during the process. This reaction starts to the proton from acid catalyst protonates the hydroxyl group of the first ethanol molecule to electrophilic. After that, the lone pair electrons of second ethanol molecule attack the electrophilic of the first ethanol molecule, and then remove the leaving group [21]. The DEE formation may be occurred by two different pathways termed the associative pathway and the dissociative pathway. Both pathways are thought to take place at Brønsted acid sites [25]. The mechanism of reaction is shown in **Figure 2.3**.

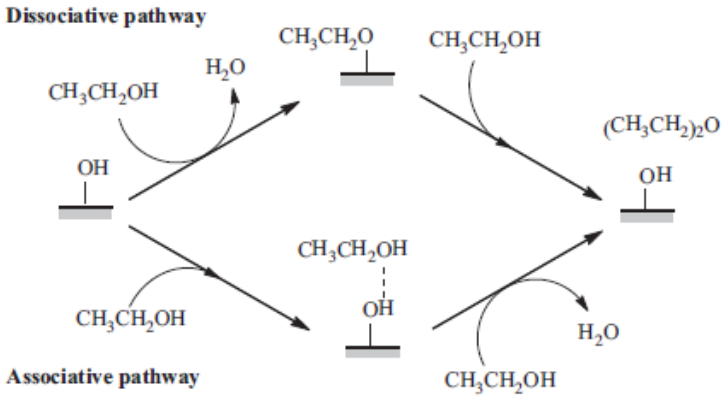

Figure 2.3 Mechanism of associative and dissociative pathways for ethanol dehydration to DEE [25].

2.2 Aluminum oxide

2.2.1 Property of aluminum oxide

Alumina or alumina oxide is compound of aluminum and oxygen which has the formula form as Al_2O_3. The structure of aluminum oxide consists of morphology and crystalline structure. There are many phases of aluminum oxide as remarked with Greek alphabet as follows: beta phase (β-Al_2O_3), gamma phase (γ-Al_2O_3), eta phase (η-Al_2O_3), chi phase (χ-Al_2O_3), kappa phase (κ-Al_2O_3), delta phase (δ-Al_2O_3), theta phase (θ-Al_2O_3) and alpha phase (α-Al_2O_3) [26]. It is known that these final properties of alumina, such as morphology, acidity, structural and textural characteristics, are affected not only by the synthesis methodology but also by the subsequent calcination conditions [13]. The phase of aluminum oxide depends on calcined temperatures of reactant (gibbsite, boehmite, and etc.). For instance, gibbsite is calcined at 280 to 650°C to obtain chi phase. When it is calcined at 750 to 1150°C, it obtains the kappa phase alumina. Boehmite is calcined at 480 to 780°C to obtain the gamma phase. Then, when it was calcined at 780 to 920°C, it obtains the delta phase [26]. **Figure 2.4** represents transition phases of alumina after calcination by different temperatures. This figure also exhibits the different types of alumina hydroxide affecting to the generation of transition phase at same temperature. Alumina hydroxide has five crystalline structures: gibbsite, bayerite, nordestrandite, diaspora, and boehmite. However, all those structures are called as bauxite [27, 28]. The name of alumina hydroxide depends on molecular form and composition between aluminum and oxygen as shown in **Table 2.1**.

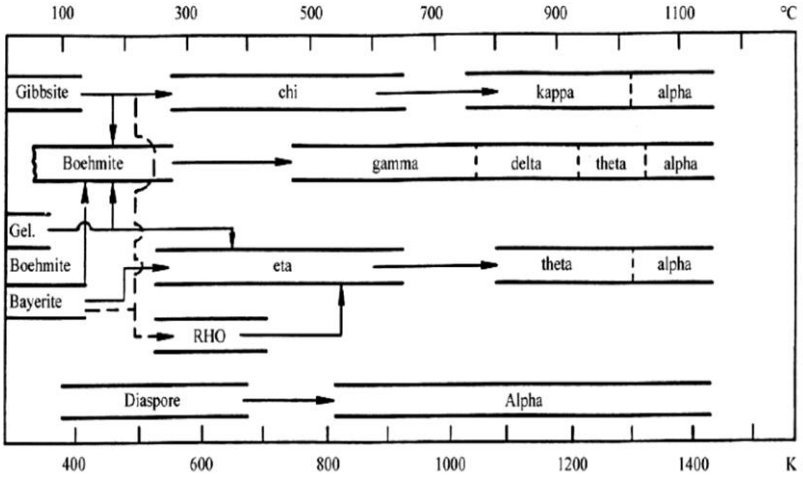

Figure 2.4 Transition phases of alumina [27].

Table 2.1 Types of bauxite [28].

Mineral Name	Chemical Composition	Accepted Standard Crystallographic Designation (1957)	Alcoa (1930)
Gibbsite/Hydrargillite	Aluminum trihydroxide	γ-$Al(OH)_3$	Alpha alumina trihydrate
Bayerite	Aluminum trihydroxide	α-$Al(OH)_3$	Beta alumina trihydrate
Nordstrandite	Aluminum trihydroxide	$Al(OH)_3$	
Boehmite	Aluminum oxide hydroxide	γ-AlOOH	Alpha alumina monohydrate
Diaspore	Aluminum oxide hydroxide	α-AlOOH	Alpha alumina monohydrate

Al_2O_3 is widely used as a common catalyst because of its fine particle size, high surface area, surface catalytic activity, excellent thermal stability, high mechanical resistance, and wide range of chemical, physical, and catalytic properties [13, 29, 30]. The surface of aluminum oxide contains acid and basic sites. The acidity and basicity of alumina can be alternated due to the existence or distinction of hydroxyl group from water molecules. The acid site on surface is Lewis and Brønsted acid site. It is

received from Al^{3+} ion and water molecule coordinated with cation, while the basicity on surface is derived from basic hydroxide group and O^{2-} anion. When aluminum oxide contacts with humidity, the water molecule has adsorbed on surface aluminum oxide and dried in air at temperature between 100 to 150°C, the water molecule is emitted, but remains hydroxyl group on surface alumina. The role of hydroxyl group is Brønsted acid site. The acid strength and concentration of aluminum oxide are low when calcined below 300°C, while calcination at 500°C decreases Brønsted acid site. The calcination temperature above 600°C results in adjacent hydroxyl group form into water molecule. Then, the water molecule releases and appears as Al^{3+} ion on surface, which is Lewis acid site. The mechanism of alumina acidity is illustrated in **Figure 2.5** [31].

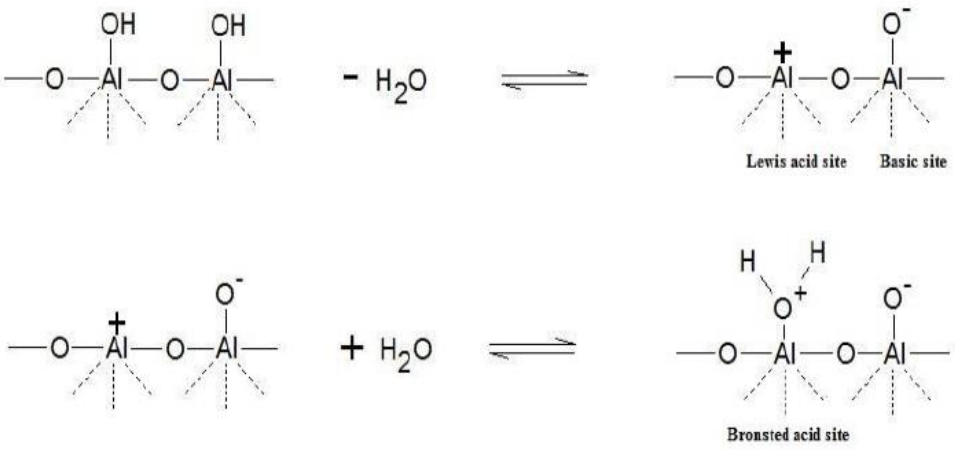

Figure 2.5 mechanism of alumina acidity [31].

2.2.2 Synthesis of aluminum oxide

Aluminum oxide can be prepared with various technique; sol–gel [32, 33], hydrothermal and sovolthermal methods [14, 15, 17, 29]. Usually, aluminum oxide is synthesized by calcination of suitable reactants but this method requires high thermal and difficult control particle size. The precipitation method is complexity and long synthesis times (washing times and aging time). Usually, metal alkoxide used as precursors for produce aluminum oxide via the sol-gel method. However, the limitation of sol-gel method is long gelation periods and high prices of alkoxide. The hydrothermal is very similar to the solvothermal method. It is difference precursor in

first step, the aqueous solution used as precursor in the hydrothermal method while the solvothermal method is usually not aqueous (but this is not always).

1.) The solvothermal method

The “solvothermal” method is a synthesis of inorganic compounds form organic compounds at temperatures between 200 to 300°C under autogenous pressure of the organics. For example, a suitable organic compounds such as ethanol, 1-butanol, toluene and etc. The advantages of the solvothermal method are control structures, grain sizes, shape distribution and morphologies by varied process conditions: reaction temperature, reaction time, solvent type, and precursor type. The prefix “solvo-” means any type of solvent for example alcohol is used as the reaction media, the reactions is called “alcohothermal” reactions. Generally, the definition of the solvothermal method is reactions at temperatures higher than the boiling point of the intermediary in liquid or supercritical media. The reaction is carried out in closed system using autoclaves.

2.) The sol-gel method

Mesoporous nanostructured materials can be easily prepared using a colloidal sol-gel. This method is based on the metallic alkoxide and water suspension. Some organic stabilizers are used to accelerate or control the rate of hydrolysis in metal alkoxides as well as improving the adherence, transparency and the quality of the corresponding films. In the sol-gel method for preparation of metal oxides and other material that is based on the phase transformation of a sol obtained from metallic alkoxides or organometallic precursors. This sol is a solution containing particles in suspension is polymerized at low temperature, in order to form a wet gel. The solvent is removed by drying the gel and the next step is a proper heat treatment. The advantages of the sol-gel method are its usefulness and the possibility that materials were obtained high purity, the preparation by sol-gel method is an easy way for the introduction of trace elements, cost of the synthesis of materials and energy savings by using low processing temperature [34].

2.3 Zeolite

The name of zeolites, which originates from the Greek words zeo (to boil) and lithos (stone), Zeolites are aluminosilicate minerals and crystalline microporous solids known as "molecular sieves" with a high specific surface area and nanometer channels that are used for many important industrial reactions such as cracking, hydrocracking and isomerization. Their crystalline structure directly controls their properties such as acidity, selectivity and stability and consequently their performance in applications such as ion exchange, separation and catalysis [35, 36]. However, in the field of catalysis: zeolites are now involved as basis components of most of the catalysts used in the production of fuels and petrochemicals; moreover they are playing an increasing role in the synthesis of intermediate and fine chemicals, as well as in pollution abatement. This is due to three main factors including molecular-size pore system of zeolites, rich variety of active sites and large number of different zeolites. Zeolites are water-aluminosilicates of natural or synthetic origin with highly structures. They are completely linked framework of tetrahedral consist of $4O^{2-}$ surrounding a cation (usually Si^{4+} or Al^{3+}), which are inerlinked through common oxygen atoms give a three dimensional network through which long channels run. The interior characteristics of zeolites channels are water molecules and mobile alkali ions, which can be exchanged with other cations. These compensate for the excess negative charge in the anionic framework resulting from the aluminum content. The interior pore system, with its atomic-scale dimension, is the catalytically active surface of the zeolites. The inner pore structure depends on the composition and the zeolites type [37].

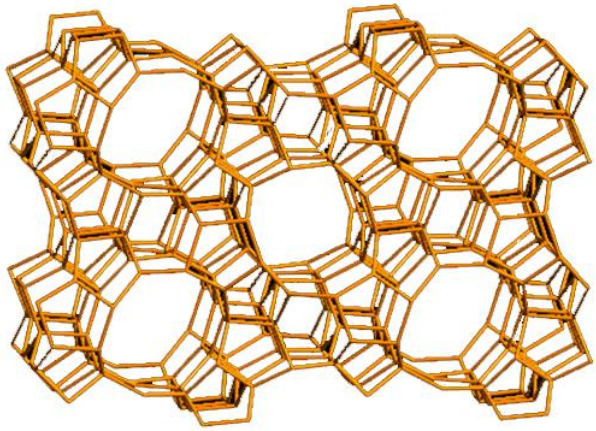

Figure 2.6 Structure of H-Beta zeolite

Zeolite beta (BEA) was synthesized in 1967 and showed high catalytic activity. The structure of BEA was only recently determined, because the crystals of BEA always contains severe structure faulting and hence shows strong diffuse scattering in diffraction patterns. The structure of BEA consists of an inter-grown hybrid of two distinct polytypic series of layers viz. polymorph A and B. Both the polymorphs have 3D network of 12-ring pores [38]. The polymorph grows as two dimensional sheets and the sheets randomly alternate between the two. BEA is of great industrial interest because of its high acidity and larger pore size. BEA has been successfully used for acid catalyzed reactions, catalytic cracking, aromatic and aliphatic alkylation. It has been shown that the acidity of BEA can be tuned by the incorporation of trivalent and tetravalent atoms (B, Al, V, Ti, Sn, Cr, Fe) into the framework positions of BEA. The isomorphous substitution creates various Bronsted and Lewis acid sites in BEA. It has been shown in the earlier studies that the Bronsted acid sites are present, both in the internal as well as on the external surface. However, this is not true for the Lewis acid sites. There are predominantly present in the framework [39]. Zeolite Beta has a three-dimensional intersecting channel system depicted in **Fig. 2.6** [38].

2.4 Promoter in catalyst

In chemistry, Promoter is act to improve the catalytic performance in a chemical reaction by adding a promoter substance added to a solid catalyst. Of course, whether a given chemical or additive acts as a promoter or a poison depends not only

on the type of catalyst, but also on the type of reaction over a given catalyst. In general, promoters can be categorized, according to their purpose, into two groups: 1) facilitating the desired reaction, i.e., increasing the activity of the catalyst, and 2) suppressing the unwanted processes, i.e., increasing the selectivity of the catalyst. Promoters of the first group are distinguished into structure forming and activating. Structure-forming promoters, as a rule, are inert substances that are present in the catalyst in the form of small particles that prevent sintering of the particles of the active catalytic phase, which prevents the reduction of the active surface during catalysis. Activating promoters can create more active sites; influence the electronic structure of the active phase, etc. Normally, chemical promoter include alkali, alkaline earth, halogen group and the noble metal catalysts such as Rh, Ru, Pd, Pt, Re, Au, and Ir that have high catalytic activity.

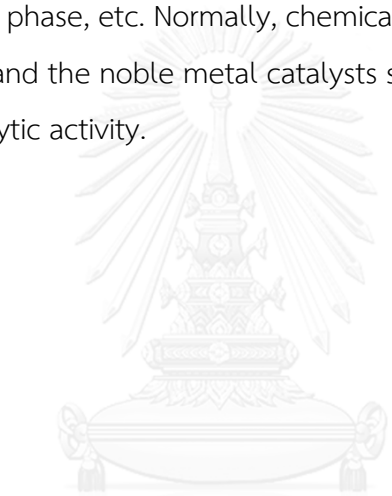

CHAPTER III
LITERATURE REVIEW

Over all catalysts, at low temperature and conversion, diethyl ether (DEE) is found as the main product, while, at higher temperature and conversion, ethylene becomes the main product.

3.1 Ethanol dehydration reaction over solid catalysts

The acidity of catalyst is important for the ethanol dehydration reaction to ethylene. Many researchers have investigated to improve and develop the catalyst for many years. Over solid acid catalysts, reaction temperature and contact time play an important role in favoring one or the other dehydration reaction [24].

In 2005, Zaki T. [8] reported catalytic ethanol dehydration, which was tested through conversion of ethanol at 200–500°C using different prepared catalysts include Fe_2O_3, Mn_2O_3, and calcined physical mixtures of both ferric and manganese oxides with alumina and/or silica gel. This work showed that the influence of reaction temperature had less effect for the ethanol conversion when compare between different prepared catalysts are used. However, the total ethanol conversion increased with increasing reaction temperature for all catalysts samples. The dehydration of ethanol to ethylene is increased with increased reaction temperature, while the diethyl ether formation is decreased. From the ethylene production selectivity, it can be explained that the highest selectivity obtained by catalysts composed of iron–manganese oxides and of iron–manganese–silica oxides. Furthermore, the ethylene production selectivity depends on the catalyst chemical constituents. This result may be concluded that the acid site on solid surface is important for ethanol dehydration to ethylene and diethyl ether.

Zhang et al. (2008) [40] this study was to compare the activity and stability of γ-Al_2O_3, HZSM-5 (Si/Al = 25), silicoaluminophosphate (SAPO-34) and Ni-substituted SAPO-34 (NiAPSO-34) as catalysts in the dehydration of ethanol to ethylene. The results showed that HZSM-5 exhibited greater ethanol conversion and selectivity to ethylene than any of the catalysts at lower temperature because strong acidic property of

HZSM-5 sample is the highest. The ethanol conversion and ethylene selectivity decreased in the order HZSM-5 >NiAPSO-34 > SAPO-34 >γ-Al_2O_3. On the other hand, the stability of catalyst, NiAPSO-34 and SAPO-34 were better than other two catalysts. NiAPSO-34 sample exhibited higher desorption temperature of both weak and strong acid sites and possessed more weak acid sites. Considering the activity and stability of the four catalysts comprehensively, NiAPSO-34 was the suitable catalyst in the dehydration of ethanol.

Madeiraet al. (2009) [24] studied the comparative three different structures of zeolites (HFAU, HBEA, and HMFI) that they have similar number of Brønsted acid sites for transformation of ethanol into hydrocarbons. The acidity and porosity of zeolites play an important role in the ethanol transformation into hydrocarbons. Over a solid acid catalyst, ethanol first undergoes a dehydration reaction on a Brønsted acid site into either ethylene or diethyl ether. The formation rate of these products depends on the acid site strength which the formation of ethylene requires stronger acid sites than that of diethyl ether. Large pore HFAU and HBEA zeolite gave mainly increasing yield of ethylene and diethyl ether with time-on-stream, due to the deactivation of the strongest acid sites and only a low quantity of C^{3+} hydrocarbons, while on medium pore of HZSM-5 zeolite was an important formation of C^{3+} hydrocarbons and very small amounts of ethylene and diethyl ether.

Bokade and Yadav (2011) [20] studied the dehydration of dilute bio-ethanol (80%m/m) over effect of three different heteropolyacid (HPA) catalysts such as dodecatungestophosphoric acid (DTPA), phosphomolybedic acid (PMA) and sodium tungstate hydrated purified (STH) supported on montmorillonite (clay). The addition of HPA supported on clay effect to increase the acidic site of catalyst. Furthermore, the acidic properties of catalyst depend on type and % loading of HPA catalysts. The report showed that the addition of HPA on clay helps to improve crystallinity of support catalysts and decrease surface area of clay with increase HPA loading. The maximum number of acid site obtained by 30% DTPA/clay and more active surface than other samples. However, the 30% DTPA/clay has shown the optimum ethanol

conversion and ethylene selectivity but the concentration of diethyl ether was found to decrease with increase in DTPA loading from 10 to 30% of the catalyst.

Martins et al. (2011) [41] reported the result of several alumina supports to evaluate the role of mesopores and macropores on the overall reaction activity by vary amount of decahydronaphthalene (DHN) adding for ethanol dehydration. The ethanol dehydration reaction, at low temperature diethyl ether is produced, while at high temperature ethylene is predominantly produced. From this study, the results were shown the addition of DHN to alumina supports effect of the different of acid properties and pore site of catalyst. At 0, 50, 60 wt% of DHN to alumina represent mesopore region while macropore region obtained from 70 wt% of DHN to alumina. For consideration of acid properties, all alumina catalyst samples have a large amount of weak acid sites. In contrast, only samples without or with lower DHN quantity owns strong acid sites. The results can be explained that strong acid site of catalyst decrease with addition of DHN. The effect of catalytic performance depended on the different of acid site concentration.

Zotov et al. (2011) [42] reported on the development of a simple technique for characterization of the weak acceptor sites on alumina-based catalysts using anthracene as the spin probe and demonstrate the existence of a good correlation between the concentration of the acceptor sites measured by this method and the ethylene formation rate during the ethanol dehydration. The modification of Al_2O_3 with sulfate and chloride ions showed the increase in the catalytic activity in ethanol dehydration because the increasing of the concentrations of the weak and strong acceptor sites. Meanwhile, the concentration of the electron donor sites decreased. They suggests that the donor sites are not related to the sites active in the ethanol dehydration. However, all the studied catalyst samples have a correlation between the concentration of the weak donor sites and the catalytic activity of the acid-modified catalysts almost passing through the origin of coordinates. So, it appears that the weak acceptor sites tested using anthracene are related to the sites active in the ethanol dehydration reaction. The results can be concluded that, the developed method for characterization of the weak acceptor sites can be useful for investigation

of the sites active in other catalytic reactions taking place on acid catalysts. Moreover, they believe that the observed good correlation between the concentration of the weak acceptor sites and the catalytic activity in solid acid catalyst for ethanol dehydration will help to understand better the nature of the surface sites.

Rahmanian and Ghaziaskar (2013) [43] used ethanol at high pressure and temperature at which it reaches supercritical conditions (the term "sc-ethanol" will be used in this study), in a continuous flow system to convert ethanol to DEE over Hydroxyapatite (HAP) and aluminum phosphate–hydroxyapatite ($AlPO_4$/HAP) catalysts. They suggested that the catalyst activity for dehydration of ethanol could be correlated with the number of strong Brønsted acid sites in the catalyst which HAP unique property of having both acidic and basic sites in a single crystal lattice. The HAP catalyst with a Ca/P molar ratio of 1.5 acts as an acid catalyst and catalyzes the ethanol dehydration while, HAP with a Ca/P molar ratio of 1.67, acts as a basic catalyst and catalyzes the dehydrogenation of ethanol to produce acetaldehyde. For this study, dehydration of ethanol to DEE was performed in the sub and sc-ethanol conditions using HAP, and $AlPO_4$/HAP as catalysts with the Ca/P and (Ca + Al)/P molar ratio of about 1.62. From this results, found that the $AlPO_4$/HAP is more active than HAP for dehydration of ethanol to DEE in sub and supercritical conditions for 41 h. They used sc-ethanol conditions for the conversion of ethanol to DEE over $AlPO_4$/HAP with the highest DEE yield, selectivity, and liquid selectivity of 75%, 96%, and 97%, respectively,

Alharbi et al. (2014) [25] investigated reaction of ethanol dehydration was studied at a gas–solid interface over a wide range of solid Brønsted acid catalysts based on Keggin-type heteropoly acids (HPAs) in the reaction temperature range of 90–220°C and focus product on the diethyl ether (DEE) formation. The catalysts was studied such as $H_3PW_{12}O_{40}$ (HPW) and $H_4SiW_{12}O_{40}$ (HSiW) supported on SiO_2, TiO_2, Nb_2O_5 and ZrO_2 with sub-monolayer HPA coverage, as well as bulk acidic Cs salts of HPW ($Cs_{2.5}H_{0.5}PW_{12}O_{40}$ and $Cs_{2.25}H_{0.75}PW_{12}O_{40}$) and the corresponding core–shell materials with the same total composition (15%HPW/$Cs_3PW_{12}O_{40}$ and25%HPW/$Cs_3PW_{12}O_{40}$, respectively) comprising HPW supported on the neutral salt $Cs_3PW_{12}O_{40}$.The result shown that the acid strength of catalysts decreases in the order: HPW > $Cs_{2.5}H_{0.5}PW$ ≈

$Cs_{2.25}H_{0.75}PW$ > HPW/SiO_2≈HSiW/SiO_2 > HPW/TiO_2> HPW/Nb_2O_5 > HPW/ZrO_2. It also decreases in the order of oxide supports: SiO_2 > TiO_2 > Nb_2O_5 >ZrO_2, which indicates increasing interaction between the HPA and support in that order. The catalyst activity depended on the catalyst acid strength, which demonstrates that Brønsted acid sites play important role in ethanol-to-DEE dehydration over HPA catalysts. It has been found that the acid strength and the catalytic activity of the core–shell catalysts HPW/$Cs_3PW_{12}O_{40}$ do not exceed those of the corresponding bulk Cs salts of HPW with the same total composition.

Matachowskiet al. (2014) [44] suggested that the catalytic activity of the potassium salts of tungstophosphoric acid as well as the bulk HPW (Potassium dodecatungstophosphates include $K_2HPW_{12}O_{40}$,$K_{2.5}H_{0.5}PW_{12}O_{40}$ and $K_3PW_{12}O_{40}$) was studied in the vapour-phase dehydration of ethanol. It has been shown that all salts were active catalysts because of the presence of protons (K2, K2.5 and HPW) as Brønsted centres and the potassium cations as Lewis centres (K3). The study was focused on the K2 and K2.5 salts because of their higher catalytic activity than that of bulk HPW which, the conversion of ethanol and selectivity to products depends on the hydration state of protons. The catalytic activity of studied samples arranged themselves in the order K2 > K2.5 > HPW > K3. Moreover, the dehydrated protons in the acidic potassium salts transform ethanol to ethylene much easier than the protons hydrated by one or two H_2O molecules present in the bulk HPW.

Phung et al. (2014) [45] the conversion of ethanol was investigated over four commercial aluminas prepared by different industrial procedures and one commercial silica-alumina. The physicochemical properties of commercial aluminas closely depend on the preparation process and impurities in catalyst. Aluminas are effective catalysts for producing ethylene from ethanol at 473-673 K. Slight differences between different aluminas are attributed mainly to different impurities present. Silica-alumina is also active in ethanol dehydration working as a Lewis acid catalyst in this reaction and Lewis acid of silica-alumina is stronger than aluminas. Its activity is similar with respect to the most active aluminas on weight base, but less on surface area basis, because of the lower density of Lewis sites and the absence of significant basicity.

Furthermore, the higher ethylene selectivity obtained by silica-alumina catalyst at high reaction temperature on the other hand diethyl ether (DEE) occurred at low reaction temperature.

Phung and Busca (2015) [46] reported that the ethanol dehydration to DEE occurs selectively at lower temperature with mechanism involving reaction of ethoxy groups with undissociated ethanol. Ethanol dehydration to ethylene occurs selectively at high temperature with an elimination mechanism via decomposition of ethoxy groups over these catalysts, but also occurs, at lower temperature. The catalytic conversion of ethanol and diethyl ether (DEE) was studied over alumina, zeolites MFI, FER and USY, silica–alumina and calcined hydrotalcite. The result shows that zeolites, alumina and silica–alumina are active for both ethanol dehydration to DEE and ethylene. Protonic zeolites are more active than alumina which is slightly more active than silica–alumina for these reactions. This result can be explained that zeolites are the most active in converting ethanol, due to their strong Brønsted acidity while alumina mostly acts as a Lewis acid catalyst. The active sites on silica– alumina reveal Brønsted sites which are different from those of zeolites. It is confirmed that the active sites of silica–alumina are different and less active than those of protonic zeolites.

Phung and Busca (2015) [6] investigated the activity of several acid catalysts in converting ethanol to ethylene. Over all catalysts in this reaction, at low temperature and conversion, diethyl ether (DEE) is found as the main product, while, at higher temperature and conversion, ethylene becomes the main product. They studied of ethanol conversion over silica-alumina catalyst different catalytic preparation. This data reported confirm that silica-aluminas are active catalysts in converting ethanol to DEE and ethylene. However, they are less active than both zeolites and γ-alumina. It is consequently confirmed that the Brønsted acidity of silica-aluminas is due to very acidic terminal silanols. For ethanol dehydration, surface ethoxy groups were found to be the active surface intermediates for both reactions. The selectivity of DEE and ethylene depends on the nature of the active site, DEE formation being more favored for lower SiO_2/Al_2O_3 ratios where Lewis sites are more frequently surrounded by alumina-like surface.

Phung et al. (2015) [47] reported on the catalytic activity of metal oxides in ethanol conversion as the addition of tungsten oxide to transition metal oxide catalysis (zirconia and titania). However, on zirconia and titania, selectivity to diethyl ether and ethylene is lowered by the production of acetaldehyde at low temperature and by the formation of higher hydrocarbons at high temperature. The result was showed that the addition of WO_3 into metal oxide are excellent catalyst for this reaction. Due to the addition of WO_3 introduces strong Brønsted acid site as an active site for ethanol dehydration on the other hand it inhibited formation of byproduct such as acetaldehyde, higher hydrocarbons. This result can be explained that the acidic species of WO_3 interaction with poison basic sites of support. This is attributed to the poisoning of basic sites and of reducible surface Ti and Zr centres, respectively, by WO_3 species. Their performances may compete with those of zeolites and alumina for conversion to both diethyl ether and to ethylene.

From the study all literature review above found that the catalysts for ethanol dehydration reaction to ethylene can be divided into 4 groups as follows:

- Phosphoric acid catalyst
- Oxide catalyst
- Molecular sieve catalyst
- Heteropolyacid catalyst

However, γ-Al_2O_3 and zeolite are mostly used as a support for catalysts because its high surface area, thermal stability, physicochemical properties having especially appropriate high surface area and porosity.

3.2 Modified zeolite as solid acid catalysts for ethanol dehydration

Among the numerous reported catalysts, HZSM-5 zeolite is the most used in the aspect of industrial application. However, it is still limited due to it is easy deactivate, low catalytic performance and low anti-coking ability. Therefore, researchers are trying to modify the catalyst structure and/or formulation in order to optimize the improvement of the catalyst stability.

Ramesh et al. (2009) [4] investigated the influence of H_3PO_4 loading on the catalytic performance of modified H-ZSM-5 catalysts for the selective dehydration of ethanol. From study found that the surface area and pore volume of H-ZSM-5 decreased with increasing the loading of H_3PO_4 because the progressive blocking of pores by PO^-_4 species inside zeolite channels. The decreasing amount of total acidity of ZSM-5 depend on P modification and the P-modification of HZSM-5 catalyst showed very high activity and stability in ethanol dehydration by selectively forming ethylene. For the P modified catalysts, diethyl ether is the only product observed at lower temperatures. The P-modified catalysts also showed higher hydrothermal stability (up to 110 h) and resistance to coke formation as compared to unmodified HZSM-5.

Zhan et al. (2010) [12] reported that the effect of catalytic dehydration of ethanol into over HZSM-5, phosphorous modified HZSM-5 and lanthanum–phosphorous modified HZSM-5 in the low temperature range from 473 K to 573 K. The result showed that the strong acidic sites of HZSM-5 were eliminated and the total acid amount was reduced after the modification with phosphorous. However, the amount and strength of weak acid and strong acid obviously increased for the 0.5%LaHZSM-5. From this study can be concluded that a little addition of lanthanum to the 2%PHZSM-5 catalyst improved the catalytic performance and anti-coking ability for ethanol dehydration to ethylene at low temperature. Because of it could be attributed to the tuned acid sites, pore structure and the synergistic interaction between the lanthanum and phosphorus. Finally, the introduction of lanthanum into phosphorus modified HZSM-5 restricted the coke formation that could lead to deactivation of catalysts and enhanced the catalysts stability.

Hanet al. (2011) [48] studied the effect of calcination temperature on the structure, acidity and catalytic performance of Mo/HZSM-5 catalyst prepared by impregnation for dehydration of ethanol into ethylene. The Mo/HZSM-5 catalyst was calcined at 450, 500, 550, 600 and 700°C and compare with calcination HZSM-5 at 500°C (HZ-500). This paper reported that the most strong acid site and total acid site were obtained by HZ-500 but Mo/HZSM-5 calcined at 500°C that is good catalytic performance for ethanol dehydration to ethylene. The results can be explained that

the modification of Mo/HZSM-5 effect to amount of weak and medium acid sites. Because of the Mo modified sample found that a new kind of acid site was generated, which may be created by the interaction between Mo species and the Brönsted acid sites. The catalytic performance and amount of weak and medium acid sites depend on the difference calcination temperature.

Takahashi et al. (2012) [49] investigated the role of phosphorus in the improvement of the initial catalytic activity and stability of ZSM-5 zeolites. From thus study, they found that the activity of the catalysts was enhanced by the addition of phosphorus, and the addition of phosphorus greatly enhanced the hydrothermal stability of the zeolites. Because of carbon deposition, which was the main cause of deactivation of the phosphorus-modified zeolites, was suppressed by H_2O produced by dehydration of ethanol. The addition of phosphorus into HZSM-5 effect to density of strong acid site of HZSM-5. The decreasing of acid site of catalyst when increase of phosphorus. Finally, they concluded that the stability of ZSM-5 catalysts during ethanol conversion was enhanced by the addition of phosphorus. Phosphorus drastically improved the hydrothermal stability of ZSM-5.

Furumoto et al. (2012) [50] considered to enhance the catalytic performance of P/HZSM-5(Ga), they have prepared several lanthanum- and phosphorous-co-modified HZSM-5(Ga) zeolites with various La/Ga and P/Ga ratios (La/P/HZSM-5(Ga)). It is well known that doping of HZSM-5(Al) with lanthanum is very effective for the improvement of hydrothermal stability as well as catalytic performance. The report was showed that the ethylene yield decreased as the La/Ga ratio increased and reached a minimum value at a La/Ga ratio of 0.05–0.1, indicating that the oligomerization of ethylene produced by the dehydration of ethanol was enhanced by doping of the P/HZSM-5(Ga) zeolite with small amounts of lanthanum. Due to the enhanced activity of the lanthanum modified P/HZSM-5(Ga) to produce ethylene is regeneration of strong acid sites. Catalytic stability of co-modified La/P/HZSM-5(Ga) exhibited enhanced catalytic stability relative to native HZSM-5(Ga) and singly modified P/HZSM-5(Ga) because of the suppression of carbonaceous deposition and elimination of gallium from the zeolite framework.

Duan et al. (2013) [51] investigated the catalytic performance of HZSM-5/SAPO-34 catalyst for ethanol to propylene. In this work, HZSM-5/SAPO-34 catalyst has been prepared by hydrothermal synthesis and physical mixture, respectively. It is known that HZSM-5 and SAPO-34 are good catalytic activity for ethanol dehydration to ethylene. They suggested the combination of HZSM-5 and SAPO- 34 modified the properties of HZSM-5/SAPO-34 catalysts, which in turn affected the catalytic reactivity of these catalysts. Especially, the chemical interaction of HZSM-5 with SAPO-34 occurred in hydrothermally synthesized HZSM-5/SAPO-34 catalyst. Therefore, hydrothermally synthesized HZSM-5/SAPO-34 catalyst showed different texture, morphology, acidity and catalytic performance from HZSM-5/SAPO-34 catalyst prepared by physical mixture. Furthermore, increasing Si/Al ratio clearly reduced the surface acidity of HZSM-5.Therefore, the acidity of HZSM-5/SAPO-34 had great influences on its catalytic reactivity. The preparation method and composition of HZSM-5/SAPO-34 catalysts affected their catalytic reactivity in the reaction. In addition, the increasing of Si/Al ratio of HZSM-5 effect to decrease yield propylene while yield ethylene increase. This results can be concluded that the catalytic reactivity and stability of HZSM-5/SAPO-34 catalysts in ethanol conversion to propylene were strongly dependent on the preparation methods, catalyst composition and reaction conditions.

Sheng et al. (2013) [11] studied the effects of the steam treatment (at temperature 400, 450, 500 and 550°C) on the mesoporosity development of HZSM-5 zeolites and on the catalytic stability in the reaction of ethanol dehydration to ethylene. They found that the steam treated catalysts at 500°C exhibit good coke-resistance, excellent catalytic stability and good selectivity for ethanol dehydration to ethylene than the parent HZSM-5 because the steam treatment created new mesopores on HZSM-5 zeolites when increasing the treatment temperature. However, the total amount of acid sites and the Brönsted/Lewis ratios of HZSM-5 zeolites decreased after steam treatment, especially for the strong acid sites. Furthermore, the newly created mesopores on catalyst during the steam treatment may accommodate

part of coke deposition, suppressing the formation of coke deposition in its inherent micropores to some extent.

Müller et al. (2015) [36] found that the dealumination (to remove 5, 10, 15, or 20 mol% of Al) of MOR, FER, and ZSM-5 zeolites can be enhanced catalytic efficiency and improved acidic properties of catalyst for alcohol dehydration. The dealumination can help to decrease catalytic deactivation by reducing coke formation in alcohol dehydration reactions while catalytic activity increase with increasing the hydrophobicity of the zeolite. Furthermore, the improvement of the acidity of the zeolites showed that it improved catalytic performance. The lower coke formation and higher conversion obtained by zeolite as least one dealuminated when compared with the parent zeolite in protonic form. The result of dealumination showed that the best sample for ethanol dehydration was H-MOR/10%. Due to it had intermediate amount of available acid sites, the highest total Si/Al ratio and one of the lowest water contents among the MOR samples. For HZSM-5 samples, H-ZSM-5/20% had one of the highest total Si/Al ratios, one of the lowest water contents and the highest crystallinity among the dealuminated ZSM-5 samples. While, H-FER/20% had the highest amount of acid sites, highest Brønsted/Lewis ratio, and weaker acid sites. Therefore, the ethanol dehydration mechanism might also be related to the presence of Brønsted acid sites.

Sujeerakulkai and Jitkarnka (2015) [18] investigated the effects of acid density and acid strength in the product distribution using various silica/alumina ratios of H-Beta zeolites (27, 37, 300). Then, H-Beta zeolites were modified with Gallium and germanium oxides (5 wt%) to study their effects on the product distribution. Many researcher to report H-ZSM-5 zeolite that it was often used as a catalyst form ethanol or ethanol dehydration because of its shape selectivity, but its pore size limits the production of large hydrocarbons. The physical properties of catalysts showed that the increasing Si/Al_2 ratio extremely reduces the surface area and pore volume of zeolites. Addition Ga_2O_3 into H-Beta zeolites to reduce the surface area and pore volume of the parent zeolites because of pore blocking by the oxide. The density and strength of the strong Bronsted acid sites are ranked in the same order as follows; B27 > B37 > B300. The total acidity of Ga_2O_3-modified zeolites with various ratios of Si/Al_2 was ranked as

follows: 5GaB37 > 5GaB27 > 5GaB300 and decreasing of Bronsted and Lewis acid sites with Ga_2O_3-modified zeolites. Moreover, the decreasing acid density and acid strength of catalysts are also found after GeO_2 loading, except on 5GeB300.

CHAPTER IV
EXPERIMENTAL

This chapter explains about the research methodology including the catalyst preparation, the experimental for ethanol dehydration reaction and the characterization of catalysts, respectively.

4.1 Catalyst preparation

4.1.1 Chemicals

Table 4.1 The chemicals used in the catalysts preparation.

Chemical	Formula	Supplier
H-beta zeolite (HBZ)		TOSOH
Aluminum isopropoxide (98%)	$[(CH_3)_2CHO]_3Al$	Aldrich
Toluene (99%)	$C_6H_5CH_3$	Merck
1-butanol (99%)	$C_4H_{10}O$	Merck
Ruthenium (III) nitrosyl nitrate solution	$Ru(NO)(NO_3)_x(OH)_y$	Aldrich
Tetraammineplatinum (II) chloride hydrate	$Pt(NH_3)4Cl_2 \bullet xH_2O$	Aldrich
Ethanol (99.99%)	C_2H_5OH	Merck
Methanol	CH_3OH	Merck
Ultra high purity nitrogen gas (99.99%)		TIG
Hydrochloric acid (37.7%)	HCl	Aldrich

4.1.2 Preparation of Al-based catalysts

Besides the HBZ catalyst, other two Al-based catalysts were used and prepared from different methods. The mixed γ-χ Al_2O_3 (M-Al) was prepared by the solvothermal method as reported by Janlamool and Jongsomjit [15]. The modified H-beta zeolite with γ-Al_2O_3 (Al-HBZ) was prepared by modified sol-gel method. First, alumina isopropoxide precursor was hydrolyzed in solution of ethanol and deionized water with volume ratio of 1:1 by stirring at 80°C for 1 h. Then, increase temperature of

solution to 90°C for 15 min. After that, the HBZ was added into the solution with HBZ to Al weight ratio of 1:3. Subsequently, add hydrochloric acid to solution and controlled pH value equal to 2.5, while stirring at 90°C for 10 h. After this step, the product became viscous. The formed gel was dried overnight at 110°C and calcined at 550°C under air flow for 2 h to obtain the Al-HBZ catalyst.

4.1.3 Preparation of modified Al-based catalysts with noble metal

The noble metal (Ruthenium and Platinum) modified H-beta zeolite catalysts were prepared by impregnation of H-beta zeolite with an aqueous solution of precursor of noble metal with 0.5 wt% loadings of noble metal. The procedure for preparation catalyst as mentioned above was calculated based on 1g of catalyst used. First, precursor of noble metal was dissolved in deionized water. Then, the solution was added dropwise into approximately 1 g of H-beta zeolite. Finally, the obtained catalyst was dried overnight in oven at 110°C and calcined in air at 500°C for 2 h, respectively.

4.2 Catalyst characterization

All catalysts were characterized by several techniques as follows:

4.2.1 X-ray diffraction (XRD)

X-ray diffraction (XRD): XRD was performed to determine the bulk crystalline phases of sample and crystal structure of an unknown. It was conducted using a SIEMENS D-5000 X-ray diffractometer with Cu$K\alpha$ (λ = 1.54439 Å). The spectra were scanned at a rate of 2.4° min^{-1} in the range of 2 theta = 10 to 90°.

4.2.2 N_2 physisorption

N_2 physisorption: Measurement of BET surface area (using the stand BET method), average pore diameter, pore size distribution (using the BJH desorption analysis) and hysteresis loop (using the adsorption-desorption isotherms) of catalysts were determined by N_2 physisorption using a Micromeritics ASAP 2000 automated system.

4.2.3 Temperature programmed adsorption (NH_3-TPD)

Temperature-programmed desorption of ammonia (NH_3-TPD): The acid properties of catalysts were investigated by NH_3-TPD using Micromeritics Chemisorb

2750 pulse chemisorption system. In an experiment, a packed quartz wool and 0.1 g of catalyst was loaded in a glass tube and pretreated at 500°C under helium flow. The sample was saturated with 15%NH_3/He. After saturation, the physisorbed ammonia was desorbed under helium gas flow about 30 min. and then the sample was heated from 40 to 600°C at heating rate 10°C/min. The amount of ammonia in effluent was measured via TCD signal as a function of temperature.

4.2.4 Scanning Electron Microscope (SEM) and Energy X-ray Spectroscopy (EDX)

Scanning electron microscopy (SEM) and energy dispersive X-ray spectroscopy (EDX) were used to determine the morphologies and elemental distribution throughout the catalyst granules, respectively. The SEM of JEOL mode JSM-6400 was applied. The EDX was performed using Link Isis series 300 program.

4.2.5 Thermo gravimetric analysis (TGA)

Thermo gravimetric analysis: TGA was performed using TA Instruments SDT Q 600 analyzer. The samples of 10-20 mg and a temperature ramping from 298 to 1273 K at 2K/min were used in the operation. The carrier gas was N_2 UHP. This technique used for determine the carbon content in the catalyst.

4.3 Reaction study in dehydration of ethanol

4.3.1 Chemicals and reagents

Table 4.2 The chemicals and reagents were used in the reaction.

Chemical	**Formula**	**Supplier**
Ethanol (99.99%)	C_2H_5OH	Merck
Ultra high purity nitrogen gas (99.99%)		TIG
High purity grade hydrogen (99.99%)		TIG
Argon		TIG

4.3.2 Reaction test

The dehydration of ethanol was carried out in a fixed-bed continuous flow microreactor made from a borosilicate glass with an inside diameter of 0.7 cm. The reaction system is shown in **Figure 4.1**. In the experiment, 0.01 g of packed quartz wool and 0.05 g of catalyst were loaded into the reactor. Then, the catalyst was pretreated in argon (60 ml/min) at 200°C for 1 h under atmospheric pressure. The reaction was carried out at temperature ranging from 200 to 400°C by feeding the vaporized ethanol into the reactor. The products were analyzed by a Shimadzu GC8A gas chromatograph with flame ionization detector (FID) using capillary column (DB-5) at 150°C.

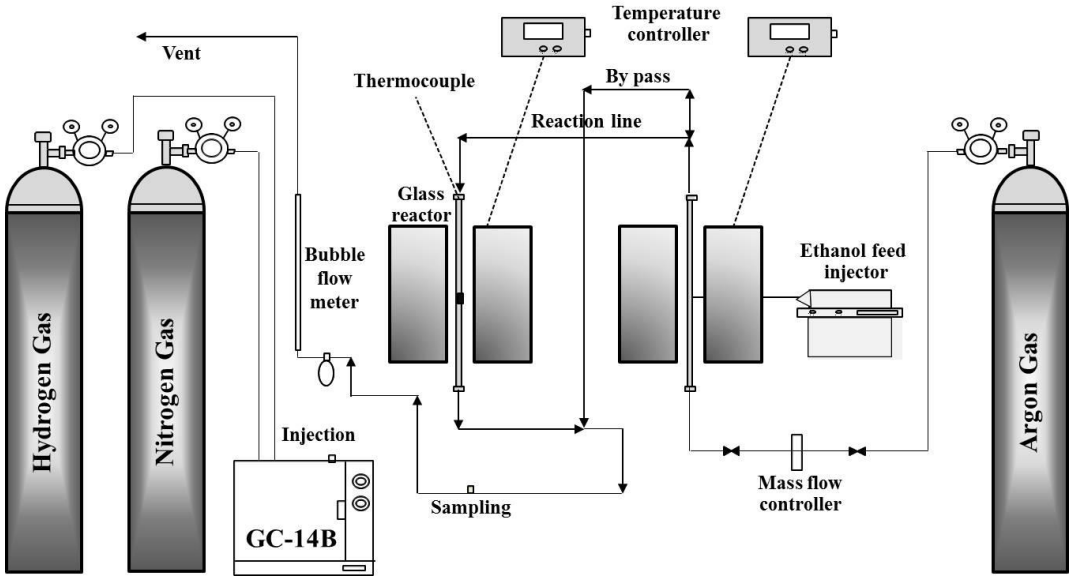

Figure 4.1 Ethanol reaction systems

1.) Reactor: The reactor tube is made from glass tube (borosilicate type) with an inner diameter 0.7 cm.

2.) Saturator: The saturator is made from glass. The role of the saturator is to produce ethanol saturated vapor from liquid ethanol which is set to bubble ethanol by feeding argon gas and providing heat by a hot-plate. The saturator is operating at atmospheric pressure.

3.) Furnace and heating cable: The furnace is provided heat for the reactor. The temperature of the furnace is controlled by interoperability of variable voltage

transformer and temperature controller. For heating cable, it is warped with the line at outlet of reactor. The heating cable is used to prevent the condensation of water dehydrated from reaction.

4.) Temperature controller: The temperature of furnace is established a set point at any temperatures in range between 200 to 400°C by temperature controller which is connected to thermocouple attached to the reactor and a variable voltage transformer.

5.) Gas controlling system: Argon is used to carrier ethanol vapor into the system. It is set with a pressure regulator, an on-off valve and mass flow controller are used to adjust the flow rate of carrier gas.

6.) Gas chromatography (GC): A Gas chromatography equipped (Shimadzu GC-14A) with flame ionization detector (FID) with DB-5 capillary column, which is used to analyze the feed and product. The operating condition for gas chromatography is reported;

- Detector: FID
- Capillary column: DB-5
- Carrier gas:Nitrogen (99.99 vol.%) and Hydrogen (99.99 vol.%)
- Column temperature
  - Initial: 40°C
  - Final: 40°C
- Injector temperature: 150°C
- Detector temperature: 150°C
- Time analysis: 8 min

CHAPTER V
RESULTS AND DISCUSSION

Chapter V describes the results and discussion on the characteristics, catalytic properties and catalytic performance of Al-based solid acid catalysts for ethanol dehydration reaction. The characteristic of all catalyst was investigated by X-ray diffraction (XRD), nitrogen physisorption, scanning electron microscopy (SEM) and energy dispersive x-ray spectroscopy (EDX), temperature programmed adsorption (NH_3-TPD) and thermo gravimetric analysis (TGA). Moreover, all catalysts were tested in ethanol dehydration reaction, considered the suitable catalysts and conditions for ethanol dehydration. In this chapter, it is divided into 3 parts. For section 5.1, the characteristics and catalytic properties on Al-based solid acid catalysts for ethanol dehydration reaction was studied. Then, section 5.2 was studied catalytic stability of Al-based solid acid catalysts for ethanol dehydration reaction. Later, the effect of the modified Al-based solid acid catalysts with noble metal was discussed in section 5.3.

5.1 Comparative study of catalytic activity of Al-based solid acid catalysts.

5.1.1 Catalyst characterization

5.1.1.1 X-ray diffraction (XRD)

X-ray diffraction technique was used to identify the different catalysts as shown in **Figure 5.1**. This figure shows XRD patterns of Al-based solid acid catalysts including the HBZ catalyst, other two Al-based catalysts were used and prepared from different methods such as the sol-gel and solvothermal method. It was found that the XRD patterns of HBZ showed the specific sharp peaks consist of 2θ at 14.6 and 22.4° [18, 52, 53] . Furthermore, the characteristic peaks of pure γ-Al_2O_3 are 46 and 67° [15] when adding γ-Al_2O_3 into HBZ to obtain the Al-HBZ catalyst, XRD peaks were occurred at 14.6, 22.4 (HBZ), 46 and 67° (γ-Al_2O_3). It indicated that the main structure of HBZ did not alter with Al addition. The addition of Al into HBZ, it was appeared that the

intensity of characteristic peak (22.4°) for HBZ decreased and suggested that the lower crystallinity of Al-HBZ was obtained. For the M-Al catalyst, the XRD peaks were appeared at 43, 46 and 67°, which can be assigned to the presence of γ-Al_2O_3 (46 and 67°) coupled with χ-Al_2O_3 (43°) as also reported by Janlamoon and Jongsomjit [15].

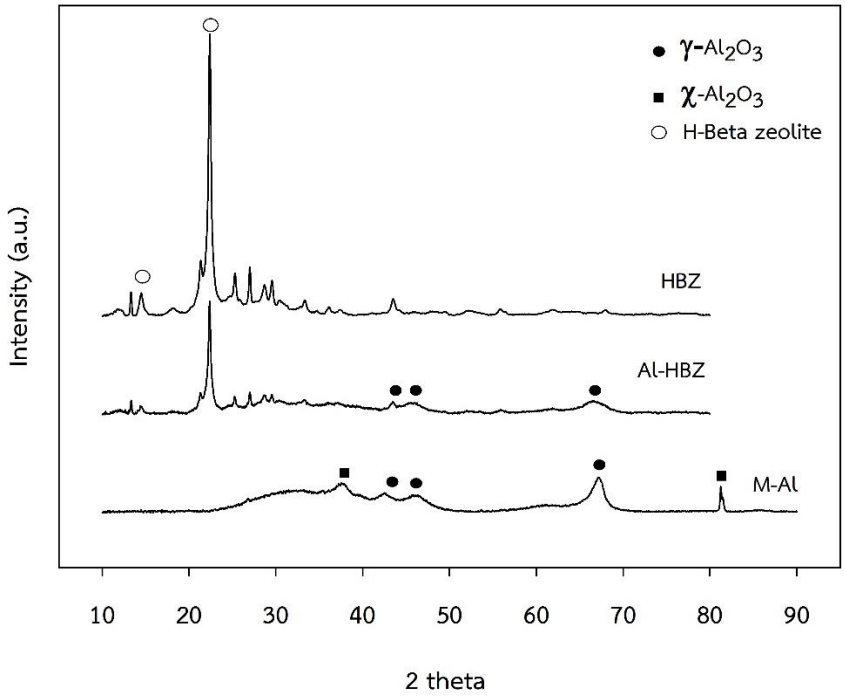

Figure 5.1 XRD patterns of all catalysts.

5.1.1.2 Nitrogen physisorption

The BET surface area and pore size diameter of all catalysts are summarized in **Table 5.1**. The BET surface area of HBZ catalyst exhibits the largest surface area of 522 m^2/g. The addition Al into HBZ (Al-HBZ) that the surface area decreased to 306 m^2/g due to occurring the pore blockage of Al in HBZ. The surface area of M-Al catalyst was lowest (ca. 195 m^2/g) when compared with HBZ and Al-HBZ. For the N_2 adsorption-desorption isotherms of all catalysts are shown in **Figure 5.2**. The pore structure of HBZ exhibited the characteristic of microporous structure according to type I classified by IUPAC (International Union of Pure and Applied Chemistry). After the addition of Al

to obtain Al-HBZ, the characteristic of type I was still observed. However, a small hysteresis loop also occurred at P/P_o around 0.4 to 0.8 indicating the presence of a small portion of mesoporous structure regarding type IV with addition of Al. This is affect to the decreasing of surface area of Al-HBZ when compared with HBZ. The lowest surface area was obtained by M-Al and it showed the pore structure of mesoporous material according to type IV that contain pore size diameter between 2 and 50 nm.

Table 5.1 Pore size diameter and BET surface area of all catalysts.

Catalyst	**Pore size diameter (nm)**	**BET Surface Area S_{BET} (m^2/g)**
HBZ	2.2	521.6
Al-HBZ	3.4	305.9
M-Al	9.0	195.4

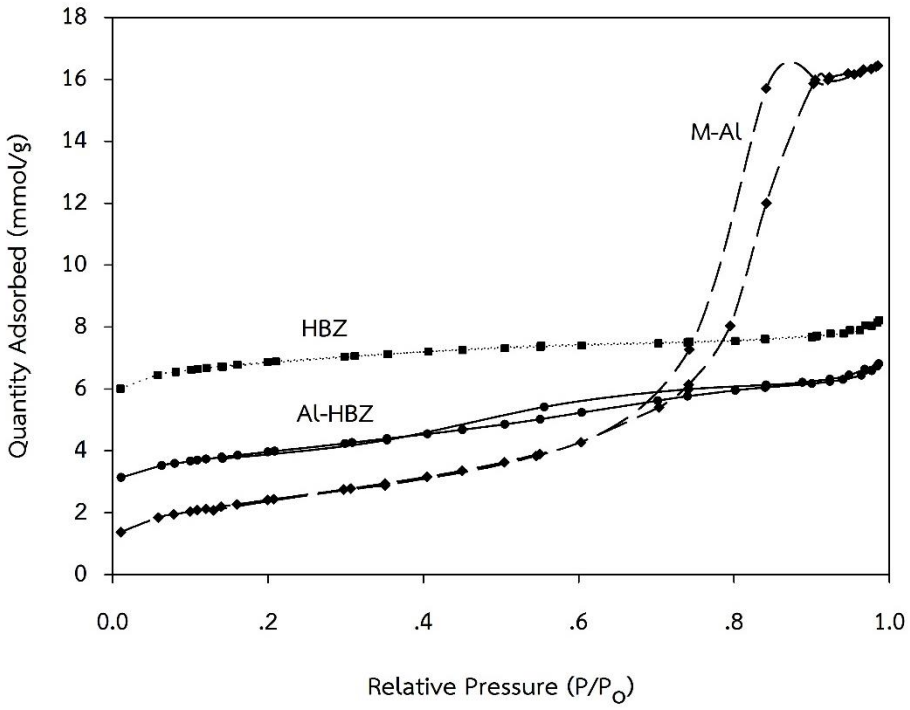

Figure 5.2 The N_2 adsorption–desorption isotherms of all catalysts.

The pore size distribution of catalysts are shown in **Figure 5.3**, which are related to the pore structure as discussed from **Figure 5.2**. The average pore size diameter as seen in **Table 5.1**. For the average pore size diameter of HBZ was ca. 2 nm (micropore). The largest average pore size diameter was obtained by M-Al (ca. 9 nm, mesopore), whereas the Al-HBZ exhibited mainly microporous structure with only a small portion of mesoporous structure as also mentioned above. It is suggested that the addition of Al into HBZ affects the catalyst resulting in losing the surface area and increasing the pore sizes diameter.

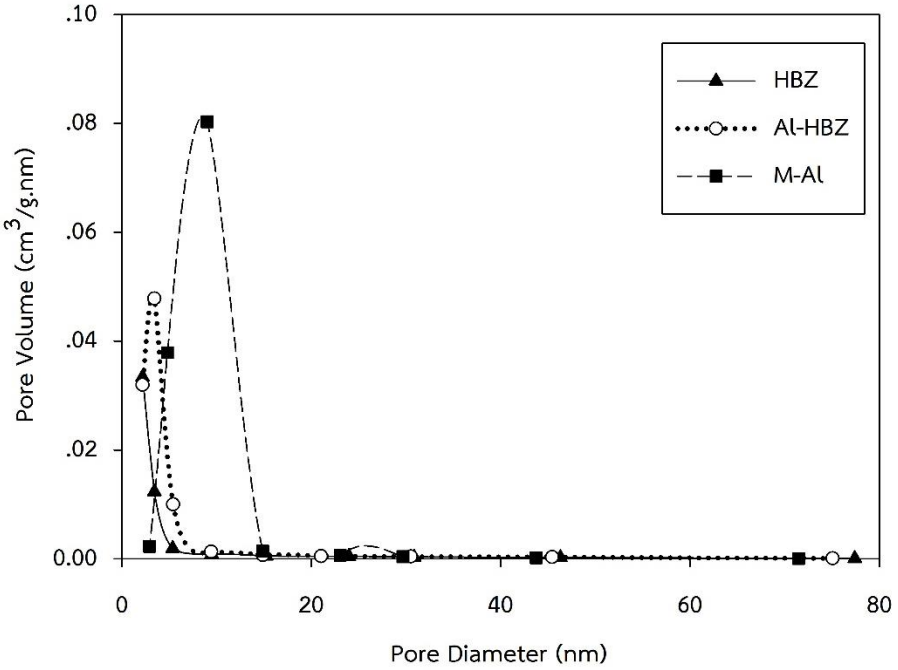

Figure 5.3 Pore size distribution of all catalysts.

5.1.1.3 Scanning electron microscopy (SEM) and energy dispersive x-ray spectroscopy (EDX)

The morphology of catalysts was observed by SEM technique as shown in **Figure 5.4**. It was found that morphologies of both HBZ and Al-HBZ showed similar spheroidal morphological features, but Al-HBZ had a rougher surface that HBZ due to Al deposition. However, the M-Al showed different morphology with more roughness.

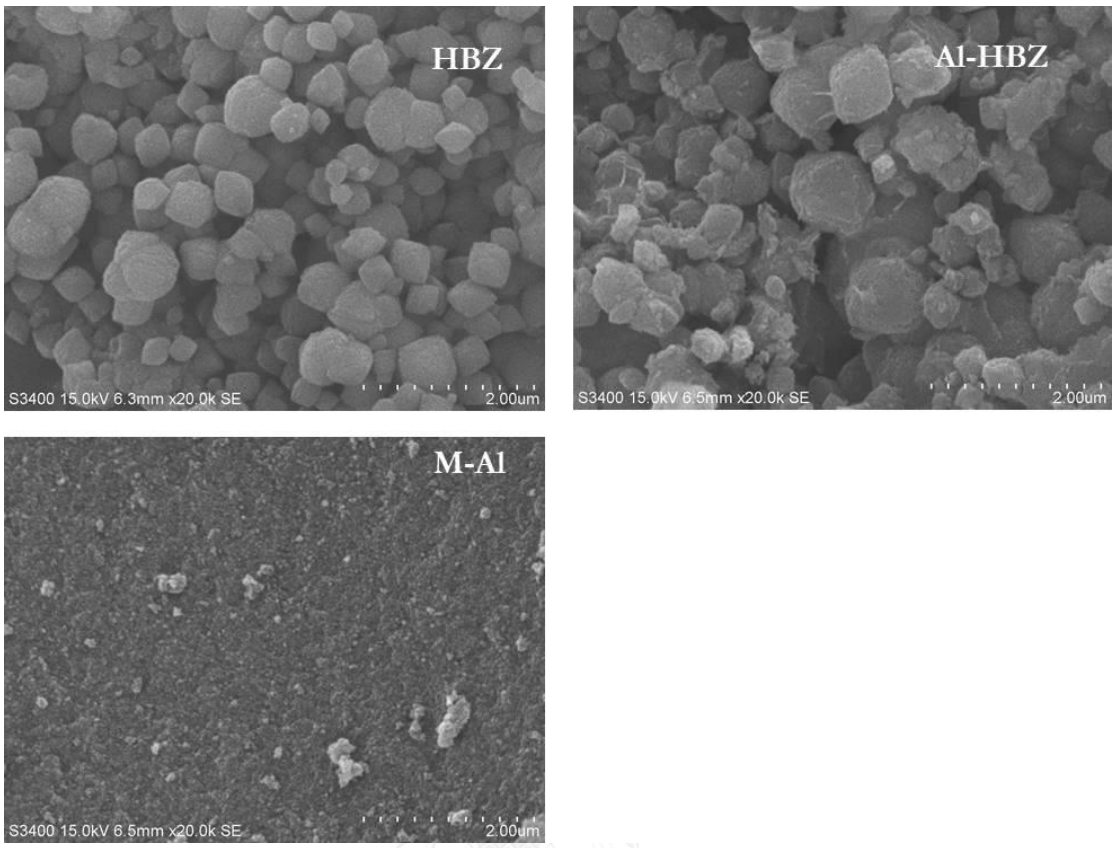

Figure 5.4 SEM images of all catalysts.

The EDX analysis was used to quantitatively measure the amounts of elemental composition on the catalyst surface. The results were shown in **Table 5.2** that it revealed the chemical composition of each catalyst. The amounts of Al present at surface were in order: M-Al > Al-HBZ > HBZ, which were reasonable. This results found that the Si/Al ratio of HBZ was the highest. The decreasing of Si/Al ratio on Al-HBZ when compared with HBZ that it occurred by the addition Al into HBZ. Furthermore, the different Si/Al ratio affects to the amount of acid sites for catalysts.

Table 5.2 Elemental composition obtained from EDX.

catalyst	Element						
	% Weight				% Atom		
	Al	Si	O	Si/Al	Al	Si	O
HBZ	3.26	44.95	51.78	13.79	2.44	32.28	65.28
Al-HBZ	32.1	22.59	45.31	0.70	24.55	16.67	58.68
M-Al	61.06	-	38.94	-	48.18	-	51.82

5.1.1.4 Temperature programmed adsorption (NH_3-TPD)

The NH_3-TPD profiles of Al-based solid acid catalysts are shown in **Figure 5.5**. It can be seen that TPD profile of each catalyst exhibited similar consisting of two groups of desorption peaks. Generally, the desorption peaks at low temperature below 250°C was attributed to weak acid sites, whereas those above 400°C was strong acid sites [11, 20, 22]. As can be seen in **Figure 5.5**, the lowest both weak acid and strong acid peaks were obtained by M-Al while HBA and Al-HBZ has a similar acid sites. These results are corresponded with amount of acid sites as shown in **Table 5.3**.

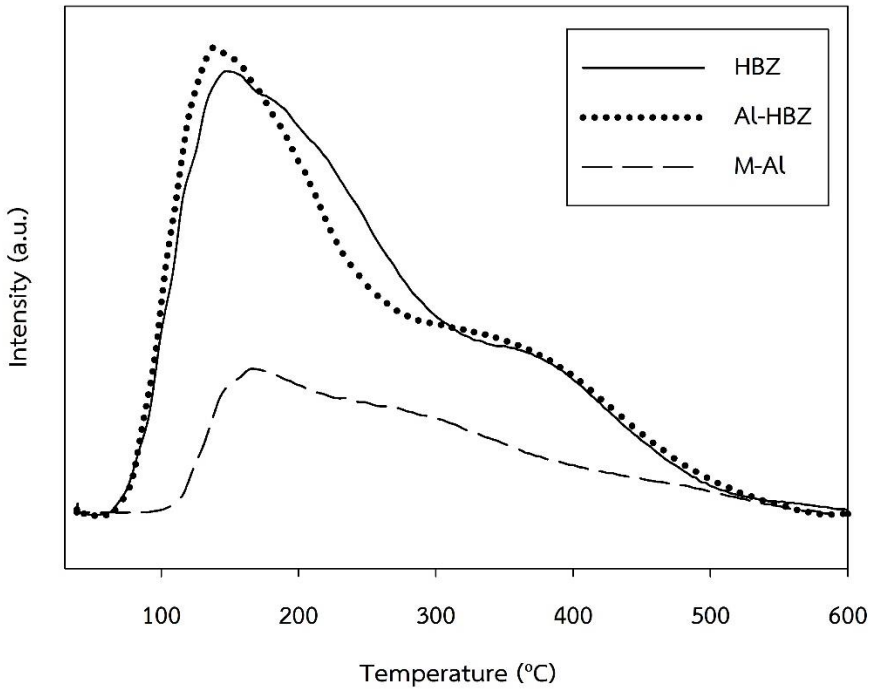

Figure 5.5 NH_3-TPD profiles of all catalysts.

The number of acid site on catalyst can be calculated by integration of desorption area of ammonia according to the Gauss curve fitting method. As **Table 5.3** was shown the amount of acidity over different catalysts. It was found that HBZ had the highest amount of weak acid sites. The addition of Al into HBZ resulted in decreased amount of weak acid site, but increased moderate to strong acid sites as well as total acidity. This can be attributed to the addition of Al possibly alter the acid distribution with different Si/Al ratios of catalysts. Moreover, the slight difference in total acidity of HBZ and Al-HBZ perhaps results from only slightly different Si/Al ratios. However, the addition of alumina into H-beta zeolite may result in slightly increased amount of medium to strong acid site. However, the amount of weak acid site, moderate to strong acid site and total acid site of M-Al were the lowest among other two catalysts. It was reported that the weak acid site is essential for the catalytic dehydration of ethanol to ethylene [22, 54]. Thus, the presence of large amount of weak acid would be beneficial to enhance the catalytic activity.

Table 5.3 The amount of acidity of all catalysts.

Samples	NH_3 desorption (μmol NH_3/g cat.)		Total acidity (μmol NH_3/g_{cat}.)
	Weak	Medium to strong	
HBZ	844.8	672.5	1517.3
Al-HBZ	813.3	731.6	1544.9
M-Al	268.7	510.0	778.6

5.1.2 Catalytic activity test

The catalytic activity of the Al-based solid acid catalysts was tested in ethanol dehydration. First, 0.05 g of catalyst was added into the fixed-bed continuous flow microreactor, then gas phase ethanol having flow rate of 60 ml/min was flowed into the reactor. The reaction was carried out in the temperature ranging from 200 to 400°C. Ethanol conversion of all catalysts apparently increased with increased temperature that were shown in **Figure 5.6**. Many researcher were reported that the catalytic activity depends on the operating temperature [9, 11, 19, 22, 23, 25, 45, 51]. Furthermore, they studied the dehydration of ethanol over acid catalyst and found that the products of ethanol dehydration reaction are ethylene (main product), DEE and acetaldehyde. At low temperature, DEE is the major product, while at high temperature, ethylene is majority. It can confirm that the operating temperature, the catalyst acidity property is an important factor influencing on the conversion ethanol and selectivity of product. Besides the results of catalytic activity were reported in terms of conversion and selectivity versus temperature profile. From these results of ethanol conversion in **Figure 5.6**, it was found that the HBZ exhibited the highest conversion of ethanol among other two catalysts for all reaction temperature. This can be attributed to the

large amount of weak acid sites present in HBZ catalyst. Considering the relationship between acidity and ethanol conversion, it was found that the acidity of catalyst plays an important role in the ethanol conversion. The ethanol conversion for Al-HBZ and M-Al was found to have a similar trend with that of HBZ, where the conversion increased with increasing reaction temperature. However, the conversion obtained from HBZ was the highest.

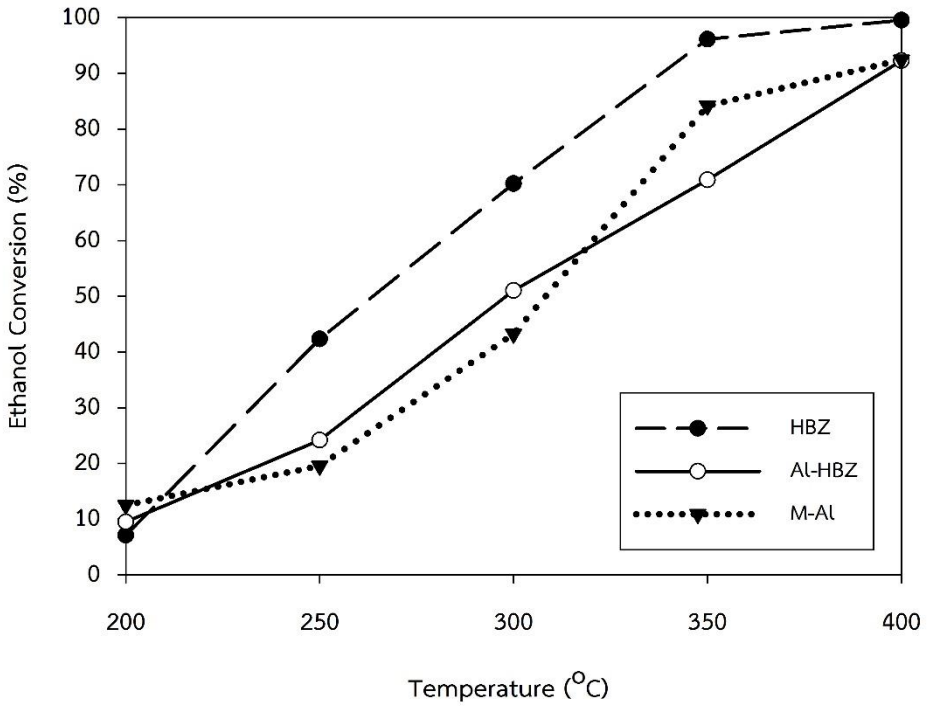

Figure 5.6 Ethanol conversion profiles for all catalysts in ethanol dehydration at different temperatures.

The ethylene selectivity of catalysts are illustrated in **Figure 5.7**. For all catalysts, the ethylene selectivity increased with increasing reaction temperature. The highest ethylene selectivity was obtained by HBZ for all reaction temperature. However, the selectivity to ethylene for all catalysts was almost equal at 400°C. On the other hand, the DEE selectivity for all catalysts apparently decreased with increasing temperature as seen in **Figure 5.8**. It can be observed that at 200°C, all

catalysts produced only DEE. It was found that the M-Al catalyst exhibited slightly higher DEE selectivity than other two catalysts. This result can be ascribed by thermodynamic properties, the reaction of ethanol to ethylene is endothermic reaction. Thus it requires high temperature. In contrast, the reaction of ethanol to DEE is exothermic reaction, therefore DEE is favor at the lower temperature.

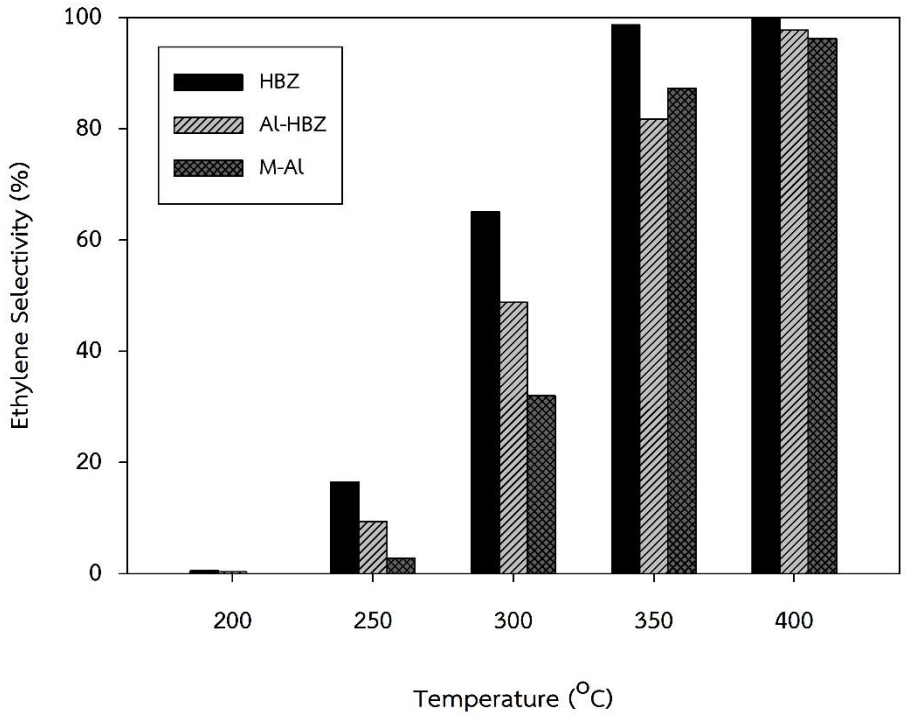

Figure 5.7 Ethylene selectivity profiles for all catalysts in ethanol dehydration at different temperatures.

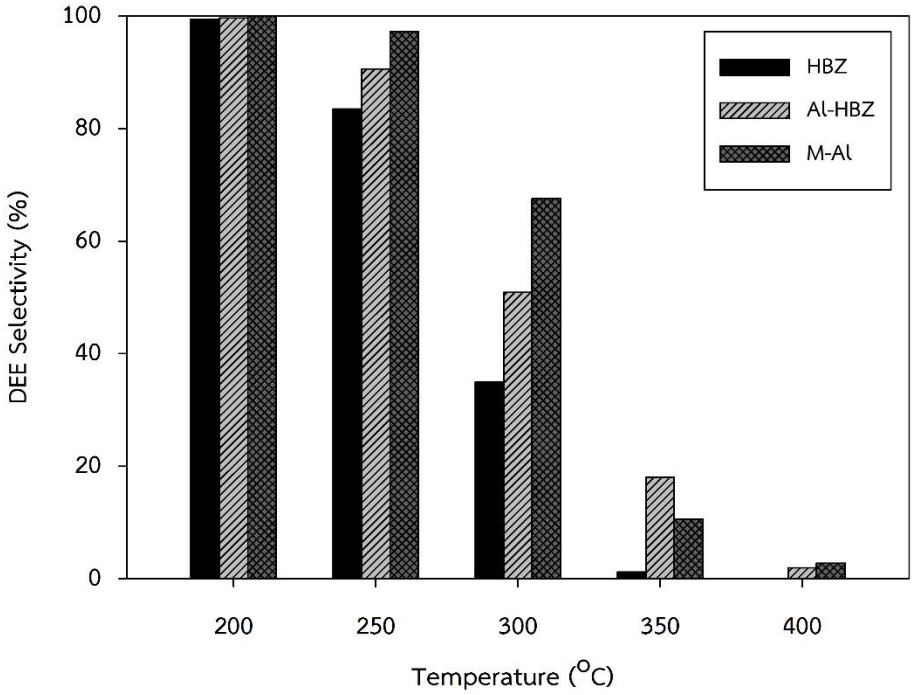

Figure 5.8 DEE selectivity profiles for all catalysts in ethanol dehydration at different temperatures.

For a comparison of the product yields obtained from catalysts. The product yields were calculated at different temperatures as shown in **Tables 5.4** (ethylene yield) and **5.5** (DEE yield). Considering for ethylene selectivity, the highest ethylene yield was obtained at 400°C indicating that high catalytic activity as well as ethanol conversion is the highest when compared with low temperature reaction. The increasing of ethanol conversion affects to increase product yield. At 400°C, the ethylene yield increased in the range of HBZ > Al-HBZ > M-Al. The DEE selectivity is also interesting. It can be observed that the highest DEE yield (35.3%) was obtained from the HBZ catalyst at 250°C. The low DEE yield was caused by low conversion. Moreover, the ethanol conversion was extremely low at 200°C. Hence, the DEE yield (product of ethanol conversion and DEE selectivity) was quite low.

Table 5.4 Ethylene yield of all catalysts.

Catalyst	Ethylene yield (%)				
	200°C	250°C	300°C	350°C	400°C
HBZ	0.0	7.0	45.7	94.8	99.4
Al-HBZ	0.0	2.3	24.9	57.9	90.2
M-Al	0.0	0.5	13.8	73.4	88.9

Table 5.5 DEE yield of all catalysts.

Catalyst	DEE yield (%)				
	200°C	250°C	300°C	350°C	400°C
HBZ	7.1	35.3	24.5	1.1	0.0
Al-HBZ	9.5	21.9	26.0	12.8	1.8
M-Al	12.5	19.0	29.2	8.9	2.5

In this section, Al-based solid acid catalysts for ethanol dehydration reaction were investigated upon the effect of the characteristics and catalytic properties. The results revealed that HBZ and Al-HBZ displays the similar acidity while M-Al exhibited the lowest acidity. All catalysts were measured upon the catalytic performance in ethanol dehydration reaction under atmospheric pressure and temperature between 200 to 400°C. The results was shown the HBZ shows the highest for both ethanol conversion and ethylene selectivity. It has the highest catalytic activity for reaction temperature range 200-400°C. This is due to the effect of acid sites. It is known that the weak acid sites of catalysts plays an important role on to enhance the catalytic activity for ethanol dehydration.

5.2 Investigation of catalytic stability of Al-based solid acid catalysts.

The experimental apparatus and set-up were similar with temperature-programmed reaction. The stability test with time on stream (TOS) of 72 h was performed for all catalysts. The ethanol dehydration temperature is 400°C for HBZ, Al-HBZ and M-Al catalysts. After pretreatment catalyst for 1 h, the ethanol with WHSV 22.9 ($g_{ethanol}g_{cat}^{-1}$) h^{-1} was fed into the reactor for 2 h before sampling the first product. Then, the effluent was collected every 4 h for 48 h and continued every 2 h for 72 h. The catalytic stability of all the catalysts is presented in **Figure 5.9** and **Figure 5.10**. Testing for stability of catalyst at 400℃ for 72 h, the result showed that Al-HBZ is lowest stability and anti-coking ability that the ethanol conversion dramatically decreased when compared with other catalysts. Due to high temperature operation leading to degradation of catalyst and high amount of carbon deposition. The catalytic stability of M-Al is constant, compared with HBZ and Al-HBZ. However, the catalytic stability of HBZ decreased slightly with reaction time after 50 h. For M-Al catalyst, it can conclude that it has a better resistance than HBZ and Al-HBZ catalysts because M-Al has the lowest weak, moderate to strong and total acid sites.

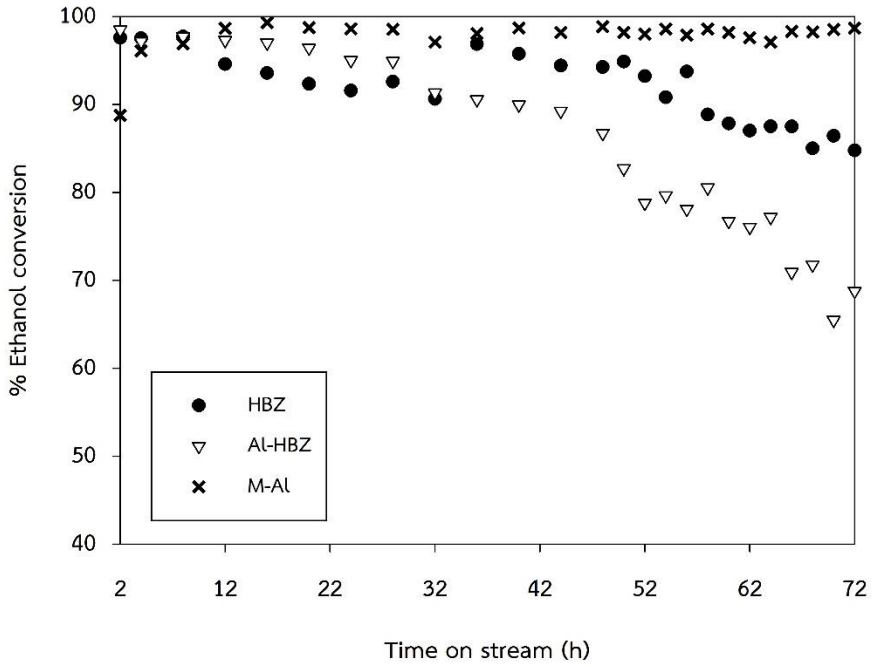

Figure 5.9 Ethanol conversion profiles for all catalysts in ethanol dehydration testing for catalytic stability.

Likewise, the ethylene selectivity decreased with increasing of reaction time. For Al-HBZ catalyst, it showed that the ethylene selectivity was extremely decreased. While, the ethylene selectivity of HBZ and M-Al have a similar trend that the results showed rather constant with increased reaction time. Due to Al-HBZ has the highest moderate to strong acid sites that it caused coke formation from further ethylene polymerization.

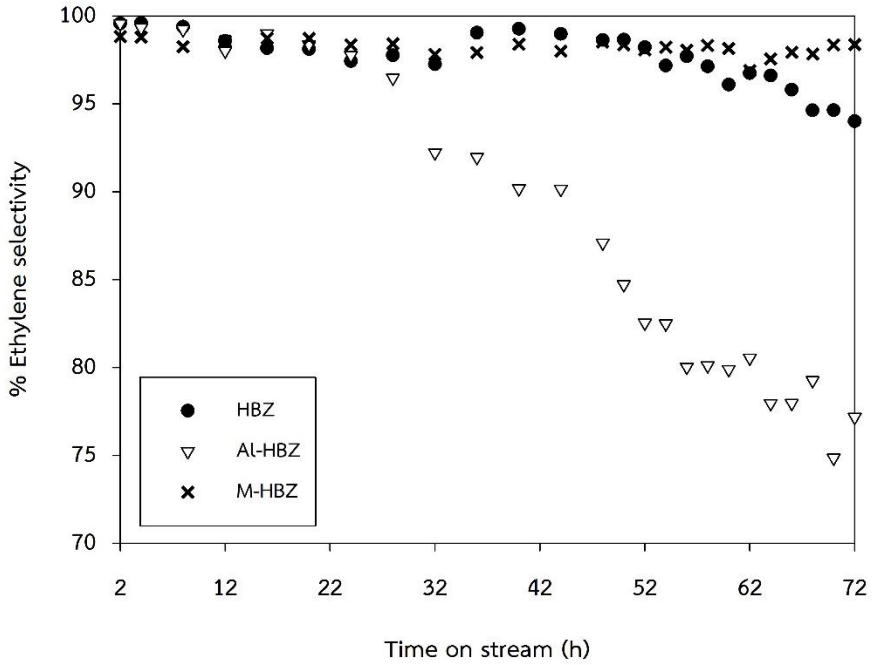

Figure 5.10 Ethylene selectivity profiles for all catalysts in ethanol dehydration testing for catalytic stability.

After testing for stability of all catalysts, they was characterized by TG analysis that determine the carbon deposition. TG profiles are shown in **Figure 5.11**, ascribed to coke deposit burning. It was found that all catalysts exhibited the similar trend of the TGA patterns. The quantitative calculation results demonstrated that the weight loss of HBZ, Al-HBZ and M-Al was 1.76%, 3.07% and 2.64%, respectively. It should be noted that the amounts of carbon deposition for each catalyst are insignificantly different. In summary, M-Al may be a good catalyst for catalytic dehydration of ethanol to ethylene with high anti-coking ability. However, TG profile of HBZ has a lower amount of coke deposition. So, HBZ may be a best activity and stability for this reaction. Moreover, HBZ can be modified to improve the catalytic activity for ethanol dehydration.

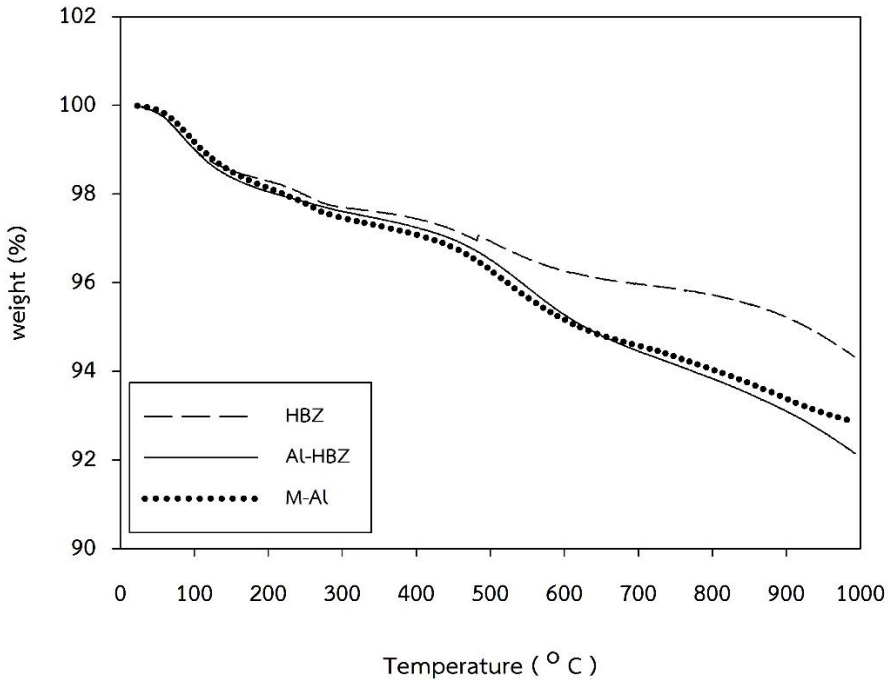

Figure 5.11 Thermal gravimetric analysis (TGA) of all spent catalysts.

5.3 Investigate modified H-beta zeolite with noble metal

5.3.1 Catalyst characterization

5.3.1.1 X-ray diffraction (XRD)

The XRD patterns for HBZ and modified HBZ catalysts are shown in **Figure 5.12**. The results confirmed that the structure of the HBZ did not destroy for Ru- and Pt-modified HBZ catalysts due to the specific peaks of H-Beta zeolites are still present. The XRD peaks of both Ru and Pt were not detected because of their highly dispersed forms [4, 18]. The XRD characteristic peaks of HBZ catalyst are present at 2θ 14.6 and 22.4° [18, 38]. The characteristic peaks for Ru- and Pt- modified HBZ catalysts are similar. After the addition of Ru and Pt into HBZ catalyst (Ru-HBZ and Pt-HBZ), it was appeared that the intensity of characteristic peak (14.6 and 22.4°) for HBZ decreased suggesting that the lower crystallinity of modified HBZ catalysts was obtained. For the

modified HBZ catalysts, the loading amount of Ru and Pt is very low. Thus, it is likely that both Ru and Pt are well dispersed on HBZ.

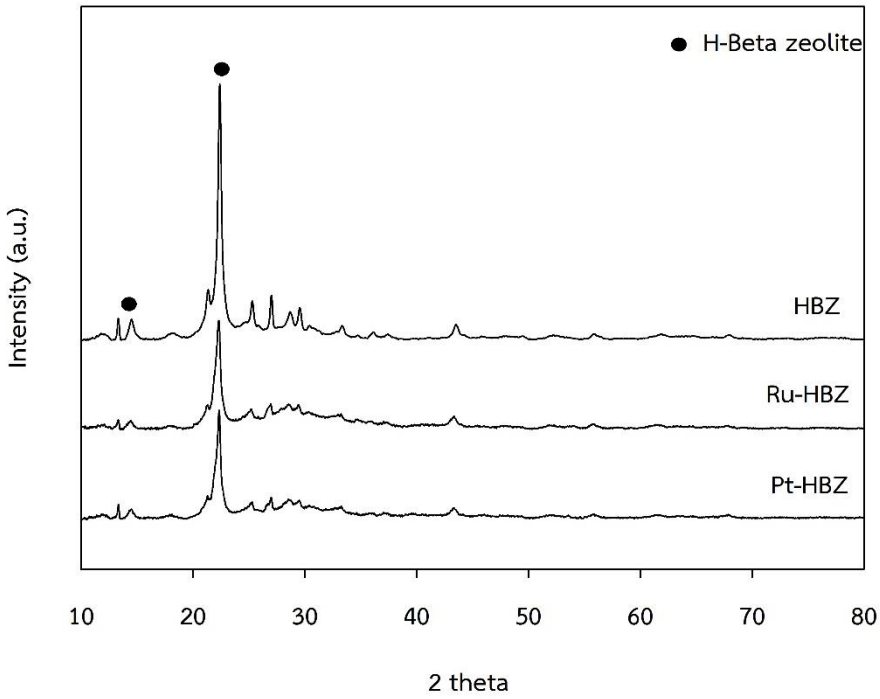

Figure 5.12 XRD patterns of all catalysts.

5.3.1.2 Nitrogen physisorption

The BET surface area and pore size diameter of all catalysts were determined by N_2 physisorption and summarized in **Table 5.6**. The surface areas of all catalysts were well above 520 m^2/g to 560 m^2/g. The BET surface area of HBZ catalyst exhibits the lowest surface area of 522 m^2/g. It indicated that the addition of Ru and Pt into HBZ were slightly higher both surface area and pore size diameter than HBZ. Due to the promoter may increase the surface for opportunities for reactants to contact and react, which would adjust the catalytic activity for dehydration of ethanol. For the N_2 adsorption-desorption isotherms for all catalysts are shown in **Figure 5.13**. The HBZ, Ru-HBZ and Pt-HBZ exhibited the characteristic of microporous structure according to type I classified by IUPAC (International Union of Pure and Applied Chemistry). Although

the Ru- and Pt- modified HBZ to obtain Ru-HBZ and Pt-HBZ, the characteristics of type I was still observed. A small hysteresis loop of the Ru- and Pt- modified HBZ suggests that mesopores exist in Ru-HBZ and Pt-HBZ catalysts, which is mainly caused from the aggregation of small crystals and leads to intercrystalline porosity [12, 48].

Table 5.6 Pore size diameter and BET surface area of all catalysts.

Catalyst	Pore size diameter (nm)	BET Surface Area S_{BET} (m^2/g)
HBZ	2.2	521.6
Ru-HBZ	3.7	541.4
Pt-HBZ	3.8	560.7

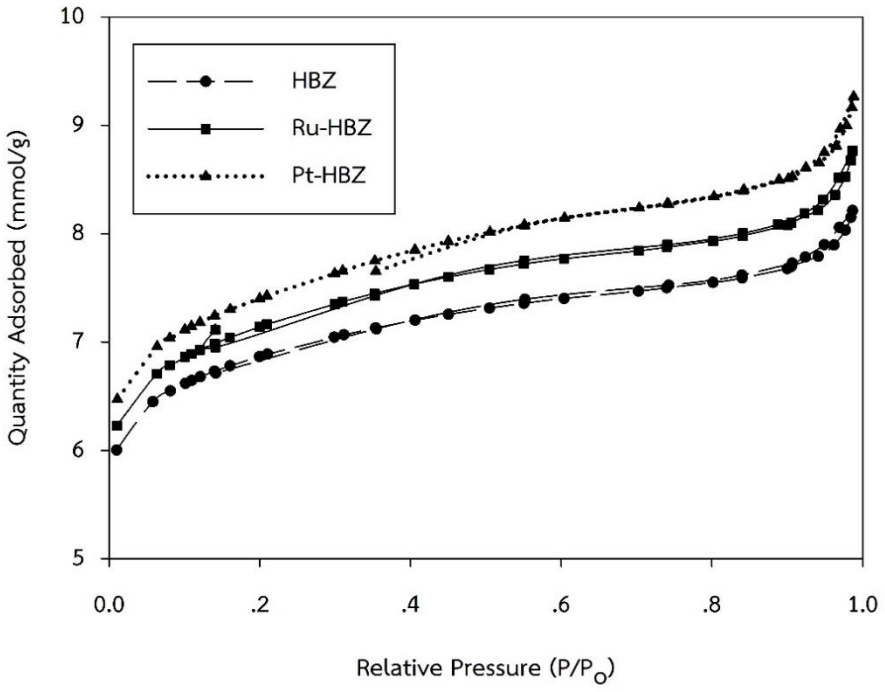

Figure 5.13 The N_2 adsorption–desorption isotherms of all catalysts.

In term of pore size distribution, all catalysts were attributed in the range of 2 to 4 nm. The pore size distribution of all catalysts are shown in **Figure 5.14**, which is related to the pore structure as discussed from **Figure 5.13**. The results show that the average pore size (**Table 5.6**) of HBZ was ca. 2.2 nm (micropore). After adding of Ru and Pt into HBZ, the average pore size diameter was slightly increased. The average pore size of Ru-HBZ and Pt-HBZ were similar at ca. 3.7 and 3.8 nm, respectively.

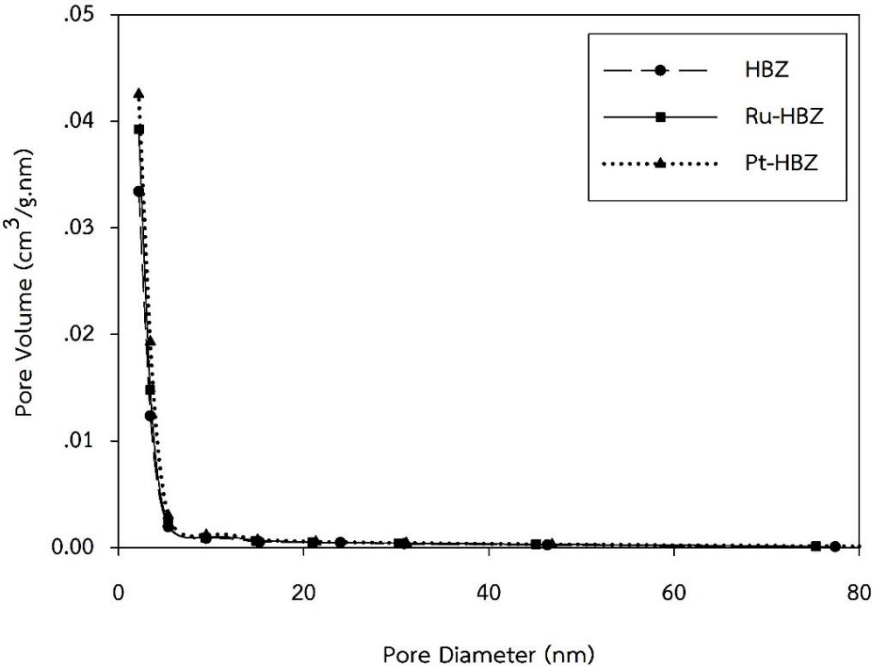

Figure 5.14 Pore size distribution of all catalysts.

5.3.1.3 Scanning electron microscopy (SEM) and energy dispersive x-ray spectroscopy (EDX)

The scanning electron micrograph images were shown morphologies of the HBZ and modified HBZ catalysts as seen in **Figure 5.15**. It can be observed that morphologies of both HBZ and modified HBZ with Ru and Pt were similar having the spheroidal shape. Elemental distribution in all catalysts can be quantitatively determined the amounts of elemental composition on the catalyst surface by EDX as

shown in **Table 5.7**. The main components of samples are O, Si, Al and noble metal (Ru and Pt). From the results, it can be estimated the amount of noble metal on surface catalysts. The amount of Ru on surface of Ru-HBZ is 0.33 wt% and 0.65 wt% Pt for surface Pt-HBZ. The detected value from EDX analysis is slightly different from the calculating loading of Ru and Pt. Due to the EDX has limit detection only about 5 micron from the outer surface, which cannot detect element in bulk of HBZ.

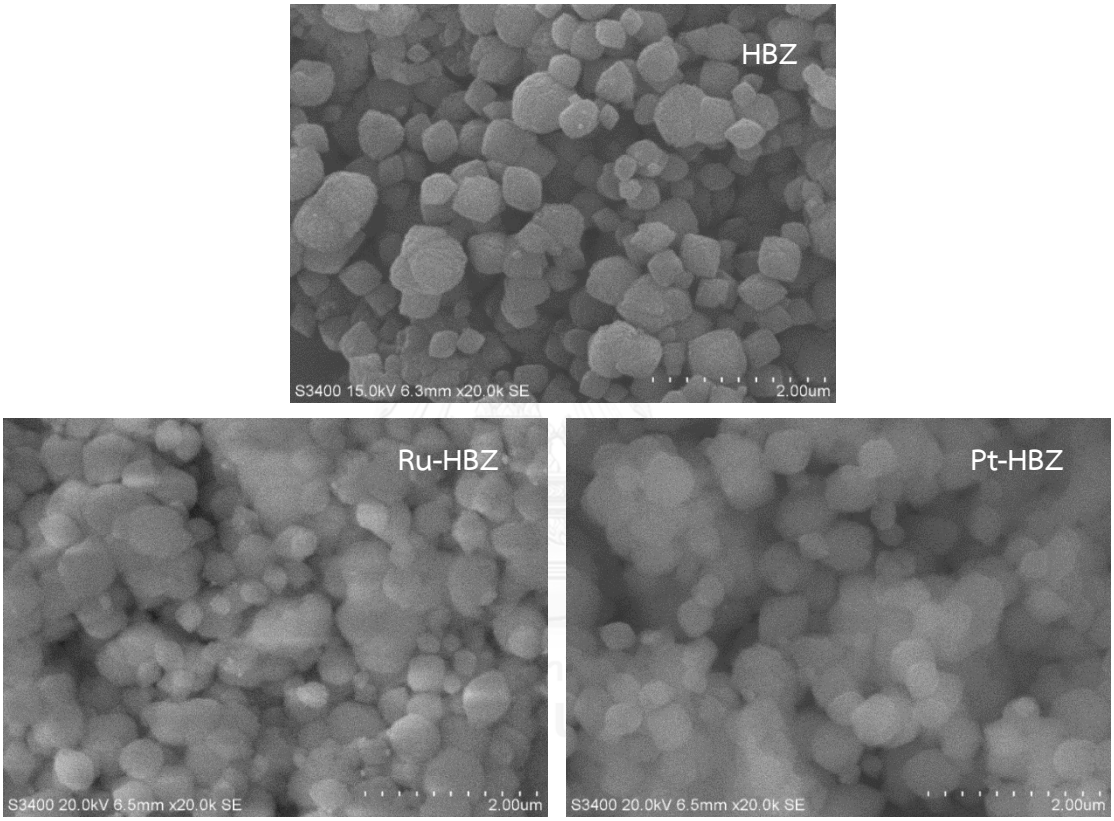

Figure 5.15 SEM images of all catalysts.

Table 5.7 Elemental composition obtained from EDX.

Catalyst	Element								
	% Weight					% Atom			
	Al	Si	O	Noble metal	Si/Al	Al	Si	O	Noble metal
HBZ	2.88	59.99	37.13	-	20.83	2.34	46.81	37.13	-
Ru-HBZ	2.61	48.14	48.93	0.33	18.44	1.98	35.18	62.77	0.07
Pt-HBZ	3.00	45.37	50.98	0.65	15.12	2.26	32.86	64.81	0.07

Figure 5.16 shows elemental distribution in all catalysts (Si, Al, O, Ru, Pt) at cross-sectional area of catalyst. The result reveals that all components inside the catalyst were well dispersed. The noble metals also exhibited good dispersion inside pore of HBZ.

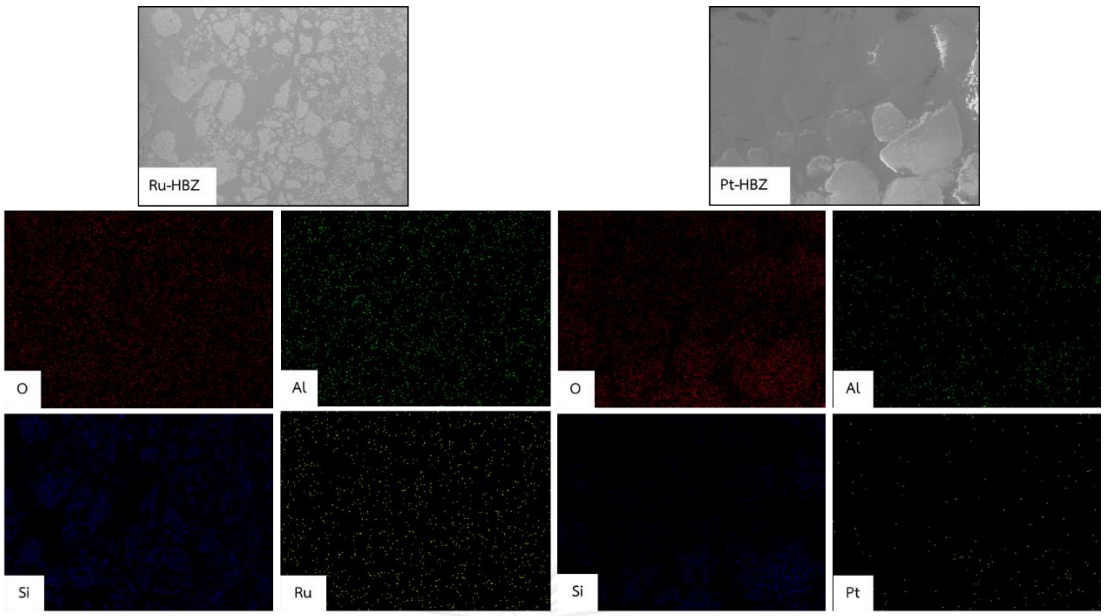

Figure 5.16 Cross-sectional elemental distribution by EDX mapping for all Ru-HBZ and Pt-HBZ catalysts.

5.3.1.4 Temperature programmed adsorption (NH_3-TPD)

The surface acidity and strength of acid site for catalysts are important factor to determine the catalytic dehydration activity of ethanol [9, 25, 54]. The acidic property of catalyst was investigated by NH_3-TPD. The NH_3-TPD profiles of all catalysts are shown in **Figure 5.17**. It can be seen that TPD profile of each catalyst exhibited similar consisting of two groups of desorption peaks. Generally, the desorption peaks at low temperature below 250°C was attributed to weak acid sites, whereas those above 400°C was strong acid sites [11, 20, 22]. The results in **Figure 5.17** reveal that weak acid and strong acid peaks were obtained by all catalysts has a similar acid sites. These results are corresponded with amount of acid sites as shown in **Table 5.8**.

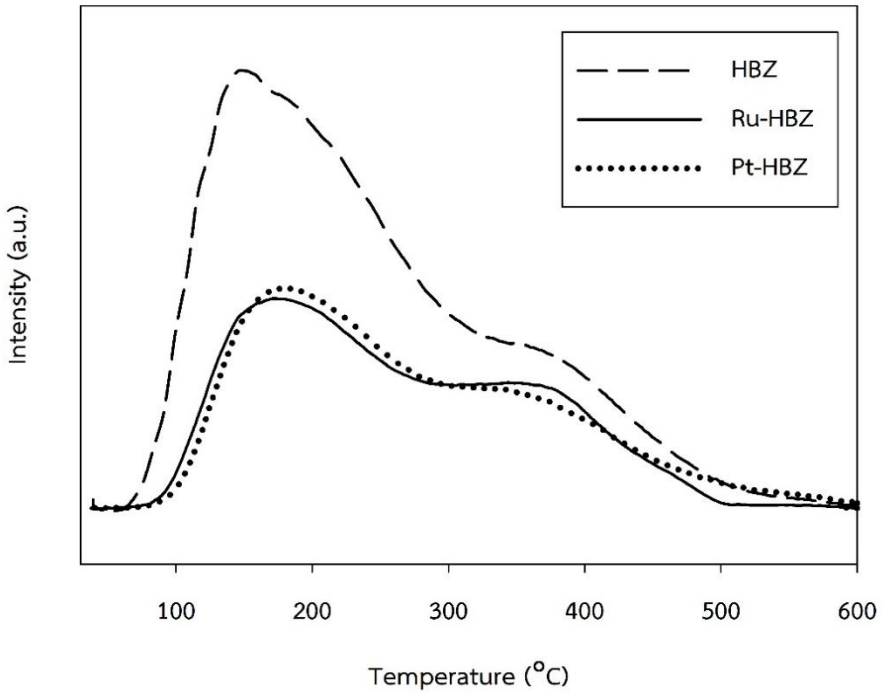

Figure 5.17 NH_3-TPD profiles of all catalysts.

Table 5.8 The amount of acidity of all catalysts.

Samples	NH_3 desorption (μmol NH_3/g cat.)		Total acidity (μmol NH_3/g_{cat}.)
	Weak	Medium to strong	
HBZ	844.8	672.5	1517.3
Ru-HBZ	695.0	624.6	1319.7
Pt-HBZ	756.4	685.8	1442.3

The number of acid site on catalyst can be calculated by integration of desorption peak area of ammonia according to the Gauss curve fitting method. As **Table 5.8** was shown the amount of acidity over different catalysts. It was found that

the trend of amount of weak acid and total acid sites were HBZ > Pt-HBZ > Ru-HBZ, whereas the amount of strong acid sites of all catalyst was slightly different. The amount of strong acid site of Ru-HBZ is slightly lower than HBZ and Pt-HBZ. This indicated that the addition of Ru and Pt over HBZ can alter the acidity of catalysts. Furthermore, the slight difference in weak, moderate to strong and total acidity of all catalysts is likely due to significant change in Si/Al ratios [6, 11, 55].

5.3.2 Catalytic activity test

From section 5.1 and 5.2, the suitable catalyst was the HBZ. It shows the best catalytic activity in both for the highest ethanol conversion and product selectivity. Therefore, the aim of this part is to investigate an improvement of catalytic activity and DEE yield for low temperature. So the noble metal (Ru and Pt) as promoter was interesting in this reaction due to previous literature. We expect that Ru and Pt may help to promote activity of the HBZ catalysts.

The noble metal (Ru and Pt) over HBZ catalysts with noble metal loading for 0.5 wt% were tested in ethanol dehydration reaction at temperature range 200-400°C upon ethanol conversion is presented in **Figure 5.18**. The result shows that all catalysts exhibited the similar behavior where the conversion of all catalyst increased with increasing of reaction temperature. At 400°C, all catalysts exhibited the highest ethanol conversion. The conversion of Ru- and Pt- modified HBZ catalysts enhanced the conversion of ethanol at temperature 250 and 300°C. However, in this results represent that the effect of Ru and Pt modification was less pronounced at high temperature (>300°C).

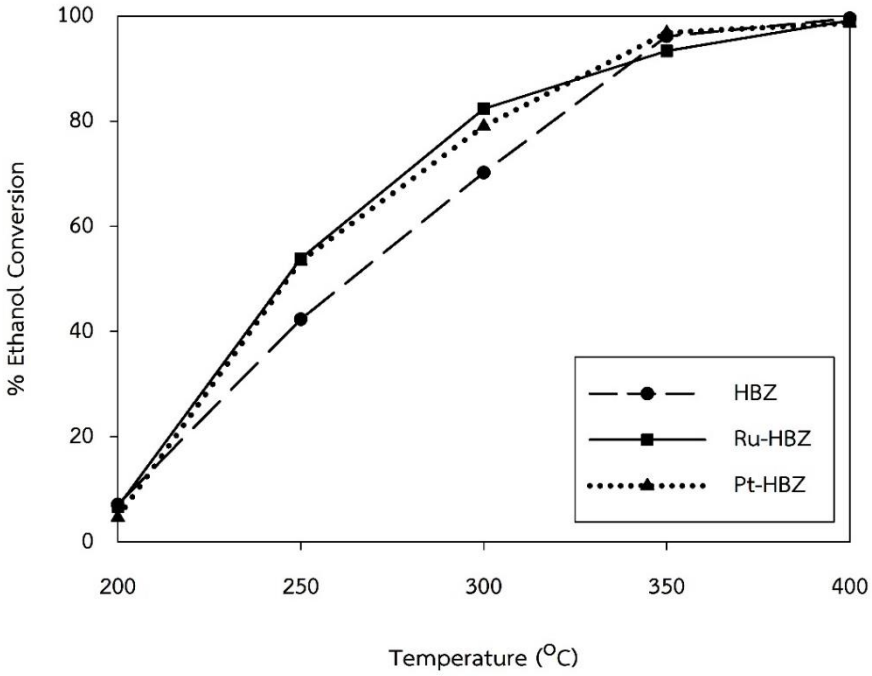

Figure 5.18 Ethanol conversion profiles for all catalysts in ethanol dehydration at different temperatures.

The ethylene selectivity of catalysts are illustrated in **Figure 5.19**. The results shows that when increasing the reaction temperature, the selectivity to ethylene continuously increased, whereas the decrease in DEE selectivity as seen in **Figure 5.20** was evident over catalysts. It can be observed that the DEE selectivity went to the maximum at low temperature (200-250°C). All catalysts exhibited the highest ethylene selectivity at 400°C. The Ru- and Pt- modified HBZ catalysts exhibited higher DEE selectivity than unmodified HBZ at 250°C and the highest of DEE selectivity was obtained from Ru-HBZ (ca. 87%).

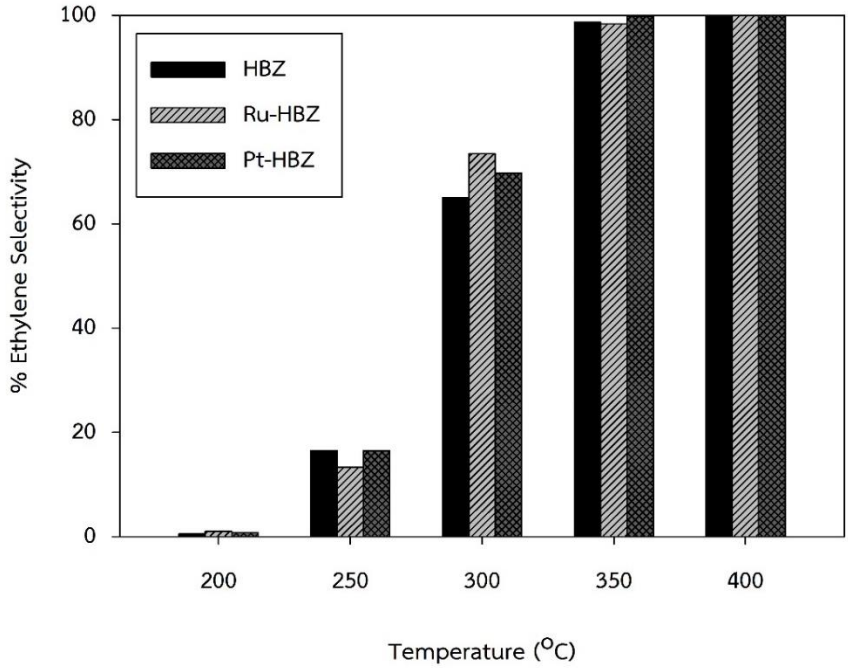

Figure 5.19 Ethylene selectivity profiles for all catalysts in ethanol dehydration at different temperatures.

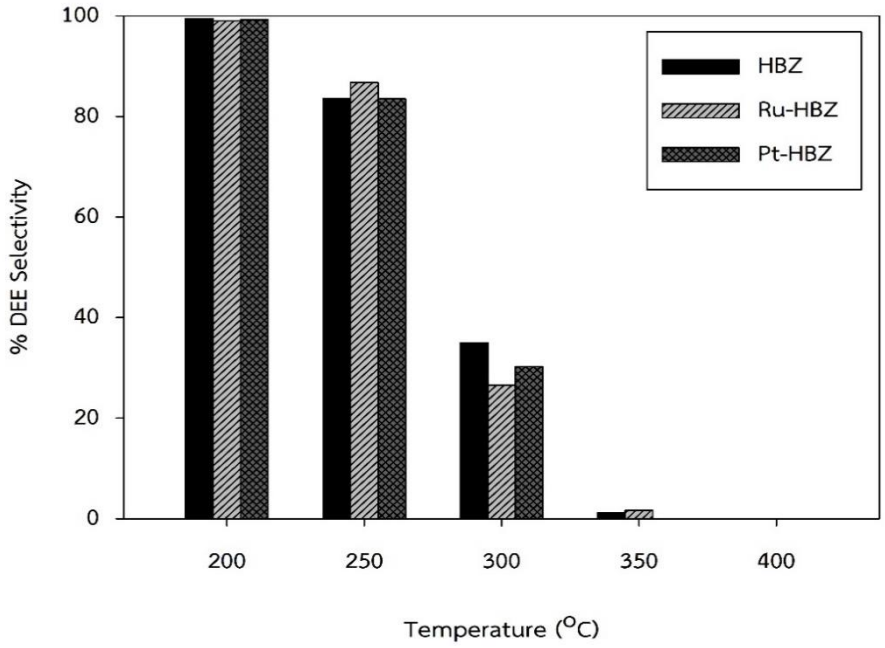

Figure 5.20 DEE selectivity profiles for all catalysts in ethanol dehydration at different temperatures.

The comparison of the product yields obtained from catalysts. The product yields were calculated at different temperatures as shown in **Tables 5.9** (ethylene yield) and **5.10** (DEE yield). Considering for ethylene selectivity, the highest ethylene yield for all catalysts was obtained at 400°C due to this temperature has the highest ethanol conversion. The increase in ethanol conversion results in increased product yield. The results show that the effect of Ru and Pt modification on HBZ can help to increase ethylene yield, especially for Ru-HBZ catalyst (ca. 60.5%) at 300°C. The ethylene yield at 300°C and DEE yield at 250°C were in the order of Ru-HBZ > Pt-HBZ > HBZ. At 250°C, DEE yields of both Ru-HBZ and Pt-HBZ were better than those of HBZ. The DEE selectivity is also interesting. It can be observed that the highest DEE yield (46.7%) was obtained from the Ru-HBZ catalyst at 250°C. Hence, it can conclude that noble metals such as Ru and Pt are able to increase catalytic activity and product yield at lower temperature.

Table 5.9 Ethylene yield of all catalysts.

Catalyst	Ethylene yield (%)				
	200°C	250°C	300°C	350°C	400°C
HBZ	0.0	7.0	45.7	94.8	99.4
Ru-HBZ	0.0	7.2	60.5	91.8	99.1
Pt-HBZ	0.0	8.8	55.1	96.6	98.6

Table 5.10 DEE yield of all catalysts.

Catalyst	DEE yield (%)				
	200°C	250°C	300°C	350°C	400°C
HBZ	7.1	35.3	24.5	1.1	0.0
Ru-HBZ	6.6	46.7	21.9	1.5	0.0
Pt-HBZ	4.6	44.6	23.9	0.2	0.0

5.3.3 DEE production

Considering the DEE production via ethanol dehydration, it has a problem that DEE is favorably formed at low temperature. However, at low temperature it results in low catalytic activity. So, this work is aimed to increase activity of catalyst by adding noble metal as a promoter. From section 5.3.2 the suitable reaction temperature were 250 and 300°C, which these condition were given the highest DEE yield. Hence, the measurement of catalytic performance of all catalysts was performed under time on stream (TOS) for 10 h at 250 and 300°C. The ethanol conversion of all catalysts at 250°C is presented in **Figure 5.21**. The highest ethanol conversion and stability during TOS of 10 h were obtained from Ru-HBZ catalyst. It should be presented that the catalytic activity of HBZ decreased with reaction time after 5 h, while the catalytic activity of HBZ of Ru- and Pt- modified HBZ increased. Thus, the Ru and Pt modification can also increase stability of HBZ catalysts.

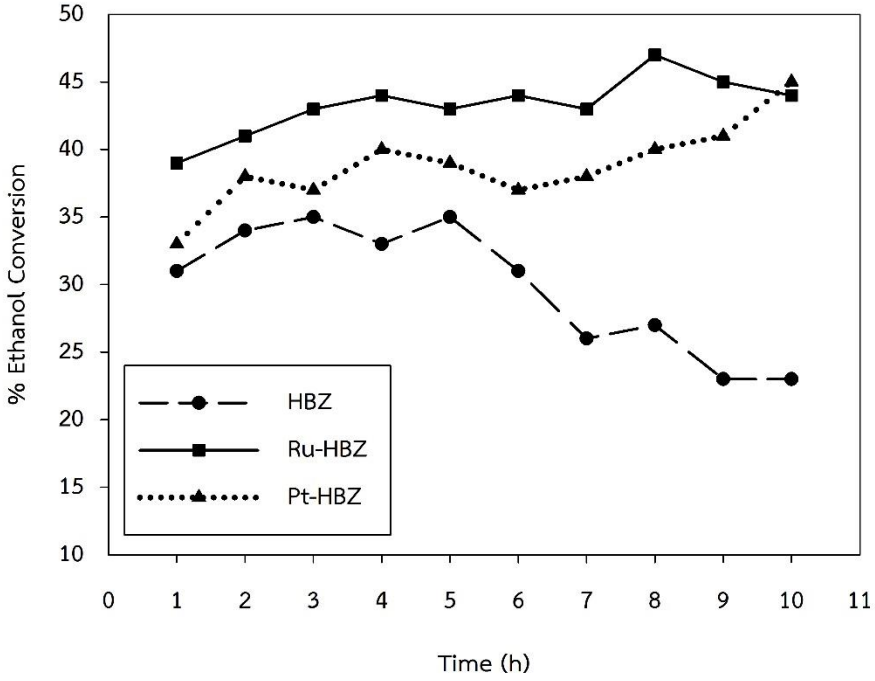

Figure 5.21 Ethanol conversion of all catalysts for time on stream at 250°C.

In addition, the catalytic dehydration of ethanol to produce DEE as a major product is investigated in this study. The result of DEE yield for all catalysts at 250°C is shown in **Figure 5.22**. After reaction time at 10 h, DEE yield of HBZ decreased from 30 to 18% indicating that remarkable catalyst deactivation. The highest DEE yield of Ru-HBZ was obtained at 35% after TOS of 10 h, meanwhile the low DEE yield was found at this condition because of low ethanol conversion.

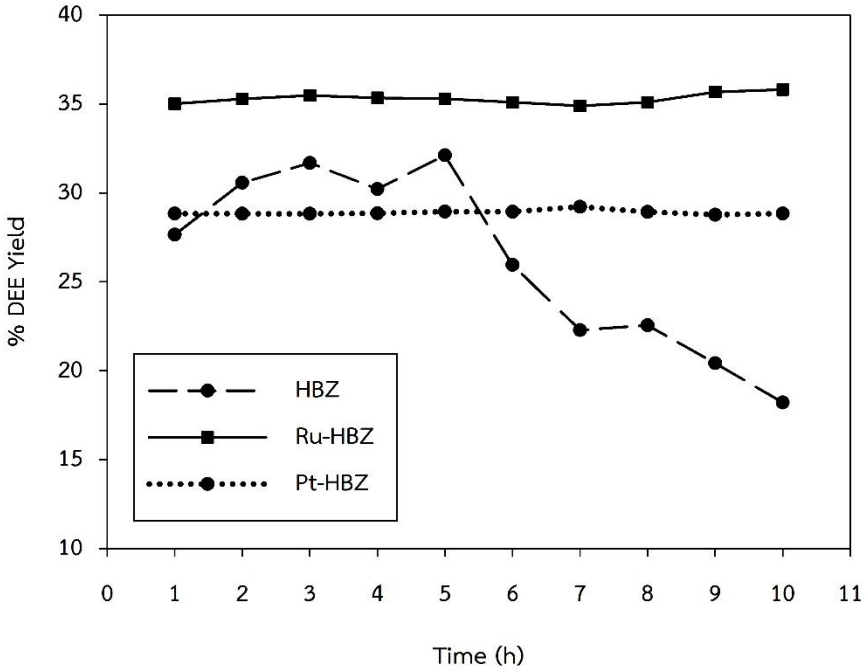

Figure 5.22 DEE yield of all catalysts for time on stream at 250°C.

The conversion of ethanol for all catalysts testing for TOS at 300°C are shown **Figure 5.23**. The results indicate that the ethanol conversion of Ru- and Pt- modified HBZ increased when compared with the unmodified HBZ. The increased conversion of ethanol over the catalysts is in the order of Ru-HBZ > PtHBZ > HBZ. The results show that DEE yield for low DEE at 300°C is illustrated in **Figure 5.24**. The DEE yield of all catalysts showed slightly different at 300°C in the range of DEE is 26-31% for all catalysts. It presents that the highest DEE yield of Ru- modified HBZ is evident, thus Ru is an important promoter for increasing of DEE yield at 250°C. Previous results also indicated that the chemical promoter is perhaps necessary for improve the DEE yield and catalytic activity [43, 47, 48, 56].

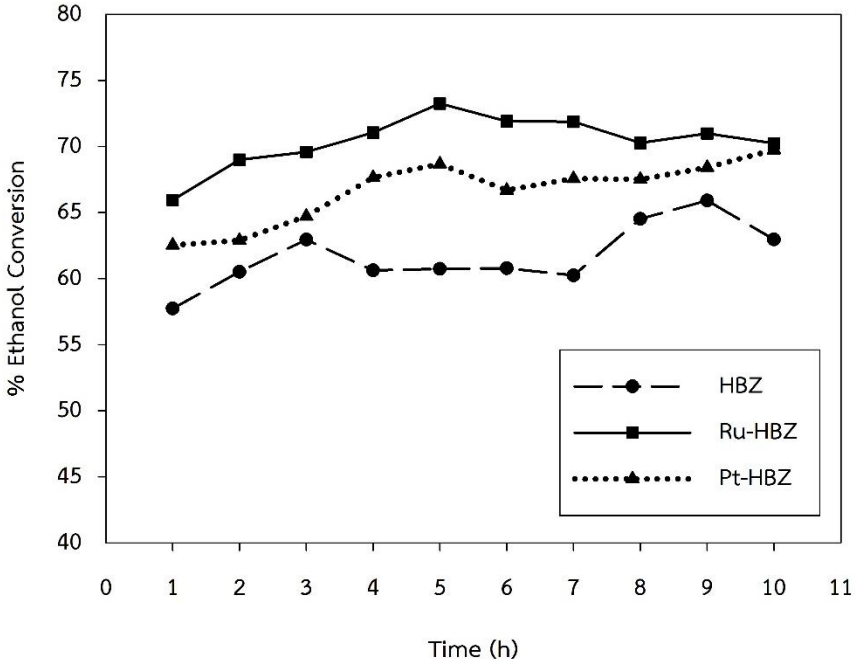

Figure 5.23 Ethanol conversion of all catalysts for time on stream at 300°C.

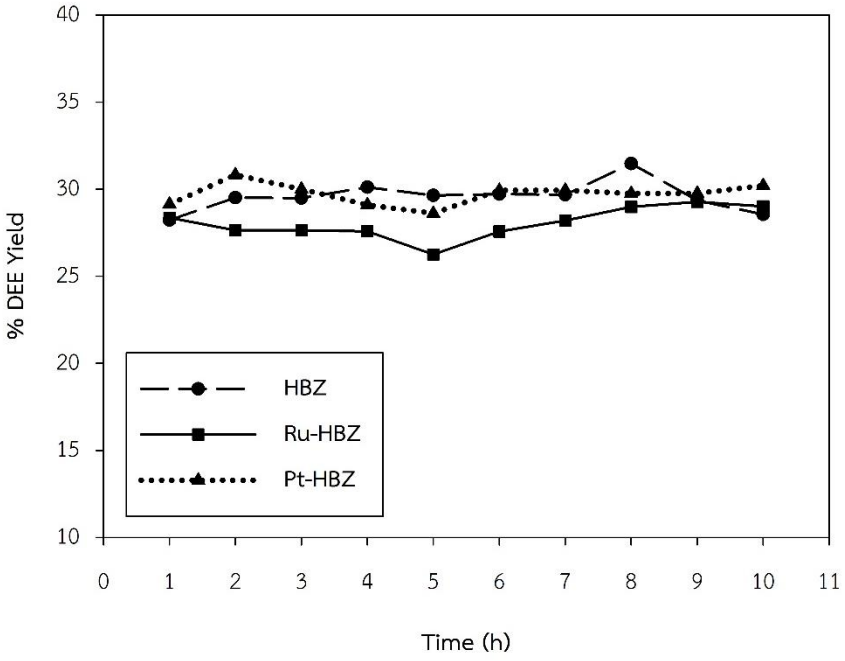

Figure 5.24 DEE yield of all catalysts for time on stream at 300°C.

To study the amount of coke deposition on catalyst after reaction, TGA measurement was performed. The TGA profiles for all catalysts at reaction temperature of 250 and 300°C are shown in **Figures 5.25** and **5.26**, respectively. It was found that all catalysts exhibited the similar trend of the TGA patterns of both reaction temperature 250 and 300°C. The weight loss below 150°C was attributed to the removal of physically adsorbed water. The weight loss at higher temperature (200-800°C) was attributed to the burning of coke deposited on the used sample surface. For the reaction temperature of 250°C, it was observed that the weight loss of HBZ, Ru-HBZ and Pt-HBZ was 1.10%, 1.81% and 1.03% (**Figure 5.25**), respectively. Moreover, the weight loss of HBZ, Ru-HBZ and Pt-HBZ was 1.45%, 1.34% and 1.70% at reaction temperature of 300°C as shown in **Figure 5.26**. Generally, zeolite catalyst has low stability, which is always occurred with coke deposition because of its large quantity of strong acid sites favoring higher hydrocarbon or polymerization. From all results, the amount of coke deposition over all catalysts showed only a slightly difference at reaction temperature of both 250 and 300°C. It demonstrated that the modification of HBZ with noble metals such as Ru and Pt enhance the catalytic activity and product yield. In addition, the modified HBZ catalysts with Ru and Pt did not affect on different amount of coke deposition, which could be responsible for the improvement of catalyst stability. Based on this study, Ru-HBZ shows the best catalytic activity with the highest DEE yield for ethanol dehydration at 250°C.

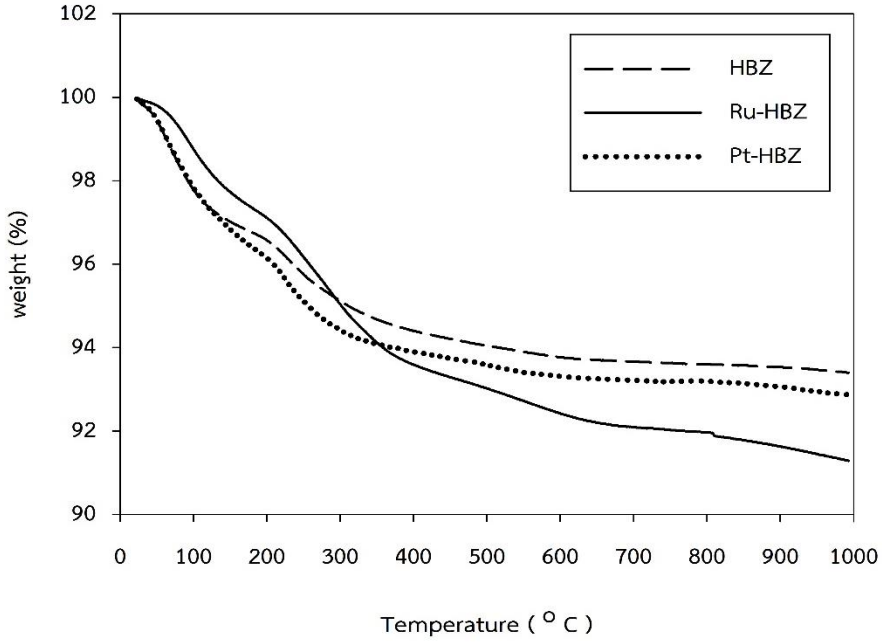

Figure 5.25 Thermal gravimetric analysis (TGA) of spent catalysts for time on stream at 250°C with 10 h.

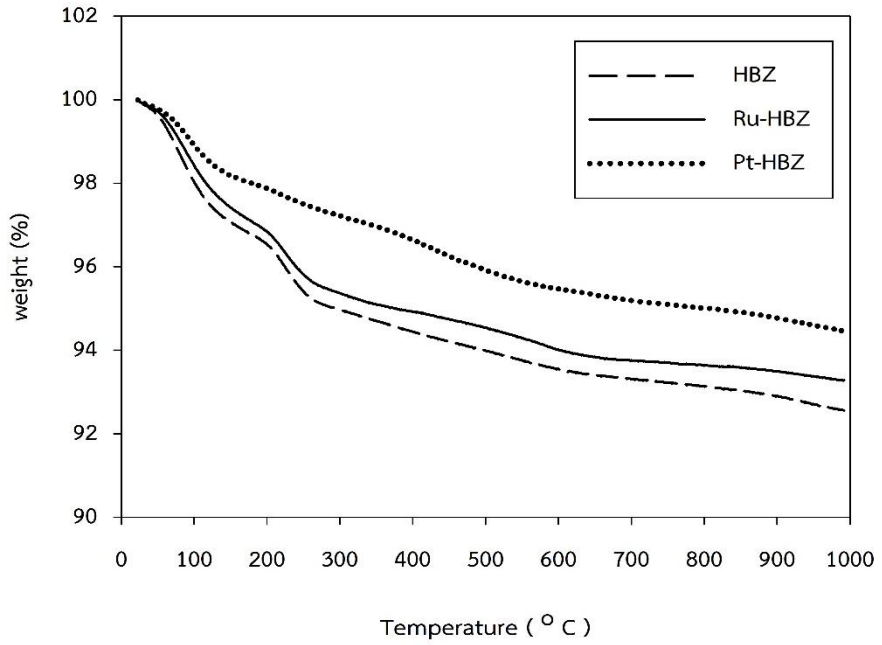

Figure 5.26 Thermal gravimetric analysis (TGA) of spent catalysts for time on stream at 300°C with 10 h.

CHAPTER VI
CONCLUSIONS AND RECOMMENDATIONS

In this research, we study in characteristic and catalytic activity of the various catalysts including H-beta zeolite, modified H-beta zeolite with γ-Al_2O_3, mixed γ-χ-phase of Al_2O_3 and modified H-beta zeolite with Ru- and Pt- catalysts, which is considered in the effect of catalytic activity and stability in ethanol dehydration reaction. Also, this chapter is summarized the results overall study in section 6.1 and the recommendations about this research in section 6.2.

6.1 Conclusions

1. For comparison catalytic activity of three Al-based catalysts including HBZ, Al-HBZ and M-Al, the HBZ catalyst is the highest ethylene yield (at high temperature, i.e. 400°C) and DEE yield (at low temperature, i.e. 250°C) because it has the highest surface area and amount of weak acid site that sites are occurred product in this reaction.

2. The catalytic performance was investigated under time on stream (TOS) for 72 h at 400°C of three Al-based catalysts. The HBZ exhibits good catalytic activity for dehydration of ethanol to ethylene. Meanwhile, M-Al exhibits good coke resistance and stability than HBZ and Al-HBZ with time on stream for 72 h duration. However, HBZ showed slightly less stability than M-Al, but HBZ has a high activity for ethanol dehydration.

3. The Ru- and Pt- modified HBZ catalyst were considered the production of DEE from ethanol dehydration under time on stream (TOS) for 10 h at 250 and 300°C. The Ru-HBZ is the most excellent catalyst for this reaction among other two catalysts. Because of the adding promoter could enhance the surface area for opportunity in increasing catalytic activity, which is suitable for ethanol dehydration to DEE. For DEE production, Ru-HBZ exhibited the highest DEE yield (ca. 35%) at 250°C. Thus, using Ru

as promoter helps for the improvement in the catalytic activity and increasing DEE yield. The high DEE yield was also obtained at low temperature. The addition of Ru over HBZ is advantage to increase the DEE yield (ca. 46.7%) at 250°C for this condition.

6.2 Recommendations

According to literature reviews, the acidity significantly affects on catalytic activity of ethanol dehydration reaction. Therefore, this research was emphasized the effect of acidity by using NH_3-TPD. However, there are several techniqes for investigation and several effects for study in order to better understanding this reaction to enhance product yield. Thus, we propose recommendation as follows:

- To indicate type of acidity (Bronsted and Lewis) with pyridine-adsorbed IR spectra.

- To consider on improvement DEE yield and catalytic activity at low reaction temperature by various amount of Ruthenium into H-beta zeolite for ethanol dehydration.

- To study another type of promoter over H-beta zeolite for increasing catalytic activity at low reaction temperature.

In order to apply for industry, we should use different sources of reactant (ethanol).

REFERENCES

[1] Kagyrmanova, A.P., Chumachenko, V.A., Korotkikh, V.N., Kashkin, V.N., and Noskov, A.S. Catalytic dehydration of bioethanol to ethylene: Pilot-scale studies and process simulation. Chemical Engineering Journal 176-177 (2011): 188-194.

[2] Bedia, J., Barrionuevo, R., Rodríguez-Mirasol, J., and Cordero, T. Ethanol dehydration to ethylene on acid carbon catalysts. Applied Catalysis B: Environmental 103(3-4) (2011): 302-310.

[3] Fan, D., Dai, D.-J., and Wu, H.-S. Ethylene Formation by Catalytic Dehydration of Ethanol with Industrial Considerations. Materials 6(1) (2012): 101-115.

[4] Ramesh, K., Hui, L., Han, Y., and Borgna, A. Structure and reactivity of phosphorous modified H-ZSM-5 catalysts for ethanol dehydration. Catalysis Communications 10(5) (2009): 567-571.

[5] Matachowski, L., Zimowska, M., Mucha, D., and Machej, T. Ecofriendly production of ethylene by dehydration of ethanol over Ag3PW12O40 salt in nitrogen and air atmospheres. Applied Catalysis B: Environmental 123-124 (2012): 448-456.

[6] Phung, T.K. and Busca, G. Ethanol dehydration on silica-aluminas: Active sites and ethylene/diethyl ether selectivities. Catalysis Communications 68 (2015): 110-115.

[7] Phung, T.K., Radikapratama, R., Garbarino, G., Lagazzo, A., Riani, P., and Busca, G. Tuning of product selectivity in the conversion of ethanol to hydrocarbons over H-ZSM-5 based zeolite catalysts. Fuel Processing Technology 137 (2015): 290-297.

[8] Zaki, T. Catalytic dehydration of ethanol using transition metal oxide catalysts. Journal of Colloid and Interface Science 284(2) (2005): 606-613.

[9] Phung, T.K., Proietti Hernández, L., Lagazzo, A., and Busca, G. Dehydration of ethanol over zeolites, silica alumina and alumina: Lewis acidity, Brønsted acidity and confinement effects. Applied Catalysis A: General 493 (2015): 77-89.

[10] Bi, J., Guo, X., Liu, M., and Wang, X. High effective dehydration of bio-ethanol into ethylene over nanoscale HZSM-5 zeolite catalysts. Catalysis Today 149(1-2) (2010): 143-147.

[11] Sheng, Q., Ling, K., Li, Z., and Zhao, L. Effect of steam treatment on catalytic performance of HZSM-5 catalyst for ethanol dehydration to ethylene. Fuel Processing Technology 110 (2013): 73-78.

[12] Zhan, N., Hu, Y., Li, H., Yu, D., Han, Y., and Huang, H. Lanthanum–phosphorous modified HZSM-5 catalysts in dehydration of ethanol to ethylene: A comparative analysis. Catalysis Communications 11(7) (2010): 633-637.

[13] Ros, S.D., Barbosa-Coutinho, E., Schwaab, M., Calsavara, V., and Fernandes-Machado, N.R.C. Modeling the effects of calcination conditions on the physical and chemical properties of transition alumina catalysts. Materials Characterization 80 (2013): 50-61.

[14] Meephoka, C., Chaisuk, C., Samparnpiboon, P., and Praserthdam, P. Effect of phase composition between nano γ- and χ-Al_2O_3 on Pt/Al_2O_3 catalyst in CO oxidation. Catalysis Communications 9(4) (2008): 546-550.

[15] Janlamool, J. and Jongsomjit, B. Oxidative dehydrogenation of ethanol over AgLi–Al_2O_3 catalysts containing different phases of alumina. Catalysis Communications 70 (2015): 49-52.

[16] Huang, B., Bartholomew, C.H., and Woodfield, B.F. Facile synthesis of mesoporous γ-alumina with tunable pore size: The effects of water to aluminum molar ratio in hydrolysis of aluminum alkoxides. Microporous and Mesoporous Materials 183 (2014): 37-47.

[17] Pansanga, K., Panpranot, J., Mekasuwandumrong, O., Satayaprasert, C., Goodwin, J.G., and Praserthdam, P. Effect of mixed γ- and χ-crystalline phases in nanocrystalline Al_2O_3 on the dispersion of cobalt on Al_2O_3. Catalysis Communications 9(2) (2008): 207-212.

[18] Sujeerakulkai, S. and Jitkarnka, S. Bio-based hydrocarbons and oxygenates from catalytic bio-ethanol dehydration: comparison between gallium and

germanium oxides as promoters on HBeta zeolites with various silica to alumina ratios. Journal of Cleaner Production (2015).

[19] Chen, G., Li, S., Jiao, F., and Yuan, Q. Catalytic dehydration of bioethanol to ethylene over TiO_2/γ-Al_2O_3 catalysts in microchannel reactors. Catalysis Today 125(1-2) (2007): 111-119.

[20] Bokade, V.V. and Yadav, G.D. Heteropolyacid supported on montmorillonite catalyst for dehydration of dilute bio-ethanol. Applied Clay Science 53(2) (2011): 263-271.

[21] Zhang, M. and Yu, Y. Dehydration of Ethanol to Ethylene. Industrial & Engineering Chemistry Research 52(28) (2013): 9505-9514.

[22] Chen, Y., et al. Dehydration reaction of bio-ethanol to ethylene over modified SAPO catalysts. Journal of Industrial and Engineering Chemistry 16(5) (2010): 717-722.

[23] Takahara, I., Saito, M., Inaba, M., and Murata, K. Dehydration of Ethanol into Ethylene over Solid Acid Catalysts. Catalysis Letters 105(3-4) (2005): 249-252.

[24] Madeira, F.F., Gnep, N.S., Magnoux, P., Maury, S., and Cadran, N. Ethanol transformation over HFAU, HBEA and HMFI zeolites presenting similar Brønsted acidity. Applied Catalysis A: General 367(1-2) (2009): 39-46.

[25] Alharbi, W., Brown, E., Kozhevnikova, E.F., and Kozhevnikov, I.V. Dehydration of ethanol over heteropoly acid catalysts in the gas phase. Journal of Catalysis 319 (2014): 174-181.

[26] Matori, K.A., Wah, L.C., Hashim, M., Ismail, I., and Zaid, M.H. Phase transformations of alpha-alumina made from waste aluminum via a precipitation technique. Int J Mol Sci 13(12) (2012): 16812-21.

[27] Santosa, P.S., Santos, H.S., and S.P.Toledob. Standard Transition Aluminas. ElectronMicroscopy Studies. Materials Research 3(4) (2000): 104-114.

[28] Shirai, T., Watanabe, H., Fuji, M., and Takahashi, M. Structural Properties and Surface Characteristics on Aluminum Oxide Powders. Ceramics Research lab 9 (2009): 23-31.

[29] Khom-in, J., Praserthdam, P., Panpranot, J., and Mekasuwandumrong, O. Dehydration of methanol to dimethyl ether over nanocrystalline Al_2O_3 with

mixed γ- and χ-crystalline phases. Catalysis Communications 9(10) (2008): 1955-1958.

[30] Bazyari, A., et al. Effects of alumina phases as nickel supports on deep reactive adsorption of (4,6-dimethyl) dibenzothiophene: Comparison between γ, δ, and θ-alumina. Applied Catalysis B: Environmental 180 (2016): 312-323.

[31] Santacesaria, E. and Gelosa, D. Basic behavior of alumina in the presence of strong acids. Industrial & Engineering Chemistry Product Research and Development 16(1) (1977): 45-47.

[32] Li, J., Pan, Y., Xiang, C., Ge, Q., and Guo, J. Low temperature synthesis of ultrafine α-Al_2O_3 powder by a simple aqueous sol–gel process. Ceramics International 32(5) (2006): 587-591.

[33] Kheirollahi, I., Abdellahi, M., Emamalizadeh, M., and Sharifi, H. Preparation and characterization of multilayer mesoporous alumina nano membrane via sol–gel method using new precursors. Ceramics International 41(10) (2015): 15083-15088.

[34] Rogojan, R., Andronescu, E., Ghitulica, C., and Vasile, B.Ş. Synthesis and characterization of alumina nano-powder obtained by sol-gel method U.P.B. Sci. Bull., Series B 73(2) (2011): 1454-2331.

[35] Chiang, H. and Bhan, A. Catalytic consequences of hydroxyl group location on the rate and mechanism of parallel dehydration reactions of ethanol over acidic zeolites. Journal of Catalysis 271(2) (2010): 251-261.

[36] Müller, J.M., et al. Solid-state dealumination of zeolites for use as catalysts in alcohol dehydration. Microporous and Mesoporous Materials 204 (2015): 50-57.

[37] Yang, S., Lach-hab, M., Vaisman, I.I., Blaisten-Barojas, E., Li, X., and Karen, V.L. Framework-Type Determination for Zeolite Structures in the Inorganic Crystal Structure Database. Journal of Physical and Chemical Reference Data 39(3) (2010): 033102.

[38] C, J., Jansena, JCreyghtonb, E., Njoa, S.L., Koningsvelda, H.v., and Bekkuma, H.v. On the remarkable behaviour of zeolite Beta in acid catalysis. Catalysis Today 38 (1997): 205-212.

[39] Shetty, S., Pal, S., Kanhere, D.G., and Goursot, A. Structural, electronic and bonding properties of zeolite Sn-Beta: A periodic density functional theory study. Theoretical Chemistry Group, Physical Chemistry Division, National Chemical Laboratory.

[40] Zhang, X., Wang, R., Yang, X., and Zhang, F. Comparison of four catalysts in the catalytic dehydration of ethanol to ethylene. Microporous and Mesoporous Materials 116(1-3) (2008): 210-215.

[41] Martins, L., Cardoso, D., Hammer, P., Garetto, T., Pulcinelli, S.H., and Santilli, C.V. Efficiency of ethanol conversion induced by controlled modification of pore structure and acidic properties of alumina catalysts. Applied Catalysis A: General 398(1-2) (2011): 59-65.

[42] Zotov, R.A., Molchanov, V.V., Volodin, A.M., and Bedilo, A.F. Characterization of the active sites on the surface of Al_2O_3 ethanol dehydration catalysts by EPR using spin probes. Journal of Catalysis 278(1) (2011): 71-77.

[43] Rahmanian, A. and Ghaziaskar, H.S. Continuous dehydration of ethanol to diethyl ether over aluminum phosphate–hydroxyapatite catalyst under sub and supercritical condition. The Journal of Supercritical Fluids 78 (2013): 34-41.

[44] Matachowski, L., Drelinkiewicz, A., Lalik, E., Ruggiero-Mikołajczyk, M., Mucha, D., and Kryściak-Czerwenka, J. Efficient dehydration of ethanol on the self-organized surface layer of $H_3PW_{12}O_{40}$ formed in the acidic potassium tungstophosphates. Applied Catalysis A: General 469 (2014): 290-299.

[45] Phung, T.K., Lagazzo, A., Rivero Crespo, M.Á., Sánchez Escribano, V., and Busca, G. A study of commercial transition aluminas and of their catalytic activity in the dehydration of ethanol. Journal of Catalysis 311 (2014): 102-113.

[46] Phung, T.K. and Busca, G. Diethyl ether cracking and ethanol dehydration: Acid catalysis and reaction paths. Chemical Engineering Journal 272 (2015): 92-101.

[47] Phung, T.K., Proietti Hernández, L., and Busca, G. Conversion of ethanol over transition metal oxide catalysts: Effect of tungsta addition on catalytic behaviour of titania and zirconia. Applied Catalysis A: General 489 (2015): 180-187.

[48] Han, Y., Lu, C., Xu, D., Zhang, Y., Hu, Y., and Huang, H. Molybdenum oxide modified HZSM-5 catalyst: Surface acidity and catalytic performance for the dehydration of aqueous ethanol. Applied Catalysis A: General 396(1-2) (2011): 8-13.

[49] Takahashi, A., Wei Xia, I.N., Shimada, H., and Fujitani, T. Effects of added phosphorus on conversion of ethanol to propylene over ZSM-5 catalysts. Applied Catalysis A: General 423–424 (2012): 162–167.

[50] Furumoto, Y., Tsunoji, N., Ide, Y., Sadakane, M., and Sano, T. Conversion of ethanol to propylene over HZSM-5(Ga) co-modified with lanthanum and phosphorous. Applied Catalysis A: General 417-418 (2012): 137-144.

[51] Duan, C., Zhang, X., Zhou, R., Hua, Y., Zhang, L., and Chen, J. Comparative studies of ethanol to propylene over HZSM-5/SAPO-34 catalysts prepared by hydrothermal synthesis and physical mixture. Fuel Processing Technology 108 (2013): 31-40.

[52] Marcus, B.K. and Cormier, W.E. Going Green with Zeolites. CHEMICAL ENGINEERING PROGRESS (1999).

[53] Nowicki, J., Mokrzycki, L., and Sulikowski, B. Synthesis of novel perfluoroalkylglucosides on zeolite and non-zeolite catalysts. Molecules 20(4) (2015): 6140-52.

[54] Xin, H., et al. Catalytic dehydration of ethanol over post-treated ZSM-5 zeolites. Journal of Catalysis 312 (2014): 204-215.

[55] Hajimirzaee, S., Ainte, M., Soltani, B., Behbahani, R.M., Leeke, G.A., and Wood, J. Dehydration of methanol to light olefins upon zeolite/alumina catalysts: Effect of reaction conditions, catalyst support and zeolite modification. Chemical Engineering Research and Design 93 (2015): 541-553.

[56] Chinniyomphanich, U., Wongwanichsin, P., and Jitkarnka, S. Sn_xO_y/SAPO-34 as catalysts for catalytic dehydration of bio-ethanol: impacts of oxidation state, interaction, and loading amount. Journal of Cleaner Production 111 (2016): 25-33.

APPENDIX

APPANDIX A

CALCULATION FOR CATALYST PREPARATION

Calculation of noble metal loading

The noble metal (0.5 wt% ruthenium and 0.5 wt% platinum) modified H-beta zeolite (HBZ) catalysts were prepared by incipient wetness impregnation method. The preparation catalyst was calculated based on 1 g of catalyst used.

-For 0.5 wt% ruthenium over H-beta zeolite was prepared as follow:

Based on 1 g of catalyst used, the HBZ catalyst contain 0.5 wt% of Ruthenium (Ru). So, the catalyst composition would be as follow:

100 g of catalyst	Consisted of ruthenium to 0.5 g
1 g of catalyst	Consisted of ruthenium to 0.005 g
Ruthenium	= 0.005 g
HBZ	= 1.00-0.005 g
	= 0.995 g

Precursors: - Ruthenium (III) nitrosyl nitrate solution ($Ru(NO)(NO_3)_x(OH)_y$)

Composition	= Ru 1.5% (typical)
Density	= 1.07 g/mL at 25°C

From precursor consisted of Ru 1.5 g in solution 100 ml

Ru 1.5 g	using Ruthenium (III) nitrosyl nitrate solution 100 ml
Ru 0.005 g	using Ruthenium (III) nitrosyl nitrate solution 0.33 ml

-For 0.5 wt% platinum over H-beta zeolite was prepared as follow:

Based on 1 g of catalyst used, the HBZ catalyst contain 0.5 wt% of Platinum (Pt). So, the catalyst composition would be as follow:

100 g of catalyst	Consisted of platinum to 0.5 g
1 g of catalyst	Consisted of platinum to 0.005 g
Platinum	= 0.005 g
HBZ	= 1.00-0.005 g
	= 0.995 g

Precursors: - Tetraammineplatinum (II) chloride hydrate ($Pt(NH_3)4Cl_2 \bullet xH_2O$) 99.99%

Molecular weight = 334.11 g/mol

$$Pt(NH_3)4Cl_2 \bullet xH_2O \text{ required} = \frac{(MW \text{ of } Pt(NH_3)4Cl_2 \bullet xH_2O) \times \text{Platinum weight require} \times 0.9999}{MW \text{ of Platinum}}$$

$$Pt(NH_3)4Cl_2 \bullet xH_2O \text{ required} = \frac{(334.11 \text{ g/mol}) \times 0.005 \text{ g of Pt} \times 0.9999}{195.84 \text{ g of Pt/mol}}$$

$Pt(NH_3)4Cl_2 \bullet xH_2O$ required=0.00853 g of $Pt(NH_3)4Cl_2 \bullet xH_2O$

APPANDIX B

CALCULATION FOR ACID SITES OF CATALYSTS

Calculation of acidity

The acidity was measured by NH_3-TPD, it can be calculated from NH_3-TPD profile as follows;

$$\text{Acidity of catalysts} = \frac{\text{mol of } NH_3 \text{ desorption}}{\text{amount of dry catalyst}} \text{---------- equation (B.1)}$$

To Calculate mole of NH_3 desorption from the calibration curve of NH_3 as follow:

NH_3 desorption (mole) = 0.0003 x A

Where, A is area under peak of the NH_3-TPD profile.

And then, we denote amount of dry catalyst as B (g.). So the equation (B.1) can be take place as equation (B.2)

$$\text{Acidity of catalysts} = \frac{0.003 \times A}{B} \text{---------- equation (B.2)}$$

APPANDIX C

CALIBRATION CURVE

Calibration curves were used calculation mole of ethanol, ethylene, DEE and acetaldehyde as shown in **Figure C.1-C.4**. The concentration of these were analyzed by the gas chromatography Shimadzu model 14A, capillary column DB-5 of flame ionization detector (FID). The conditions uses in GC are presented in **Table C.1**

Table C. 1 Conditions use in GC-14A.

Parameters	Condition
Width	5
Slope	100
Drift	0
Min.area	300
T.DBL	1000
Stop time	8 min
Atten	2
Speed	3
Method	Normalization
SPL.WT	100
IS.WT	1

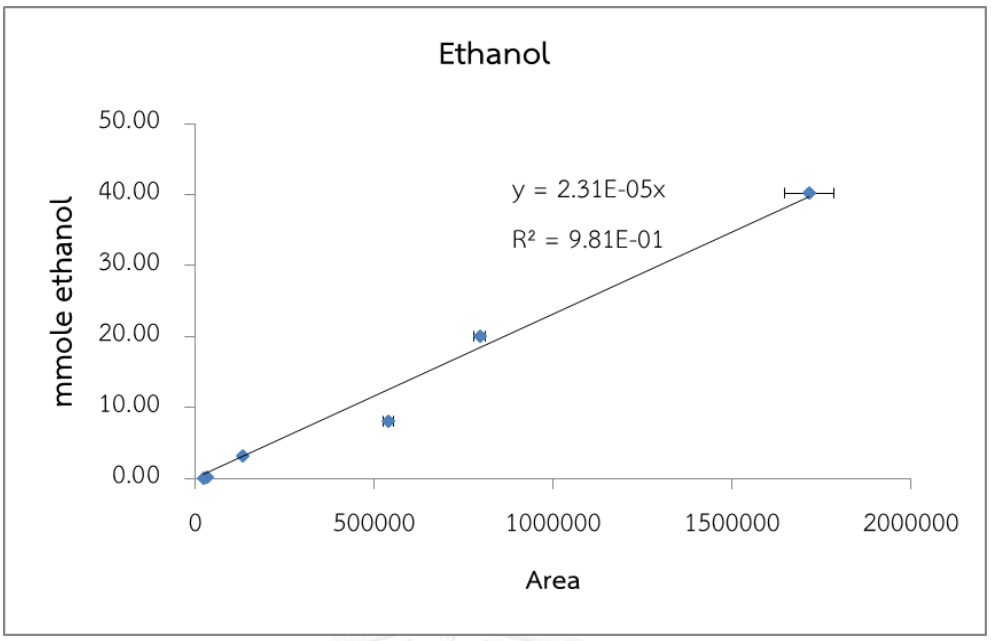

Figure C.1 The calibration curve of ethanol.

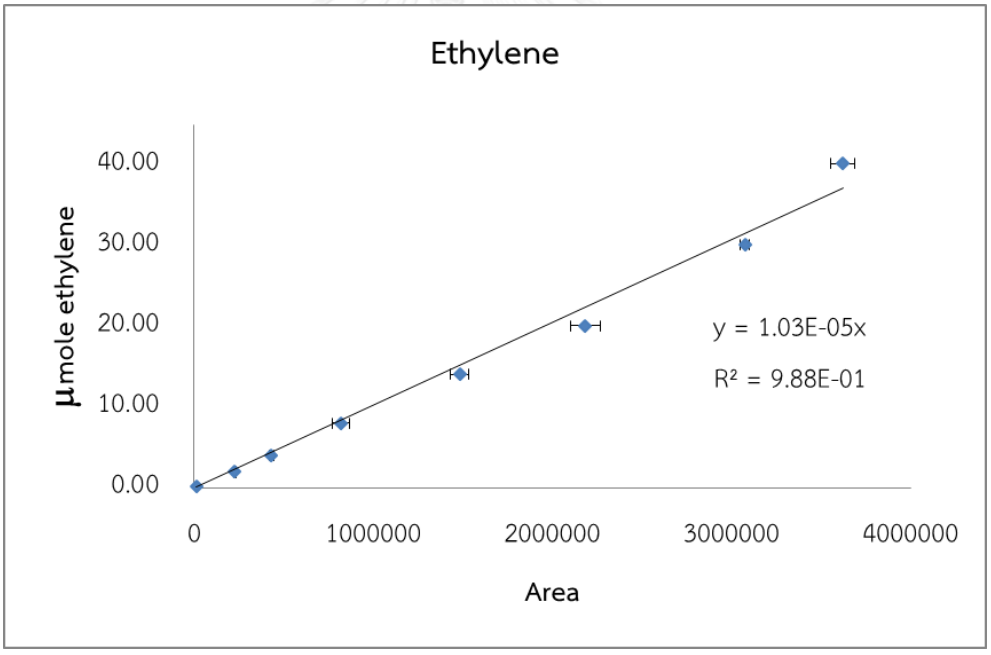

Figure C.2 The calibration curve of ethylene.

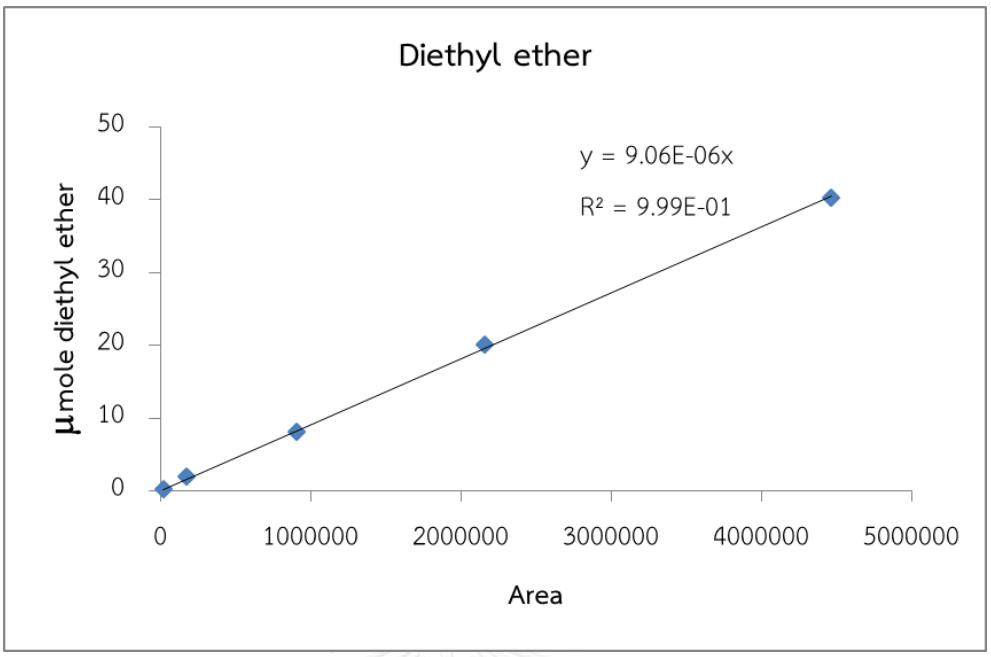

Figure C.3 The calibration curve of DEE.

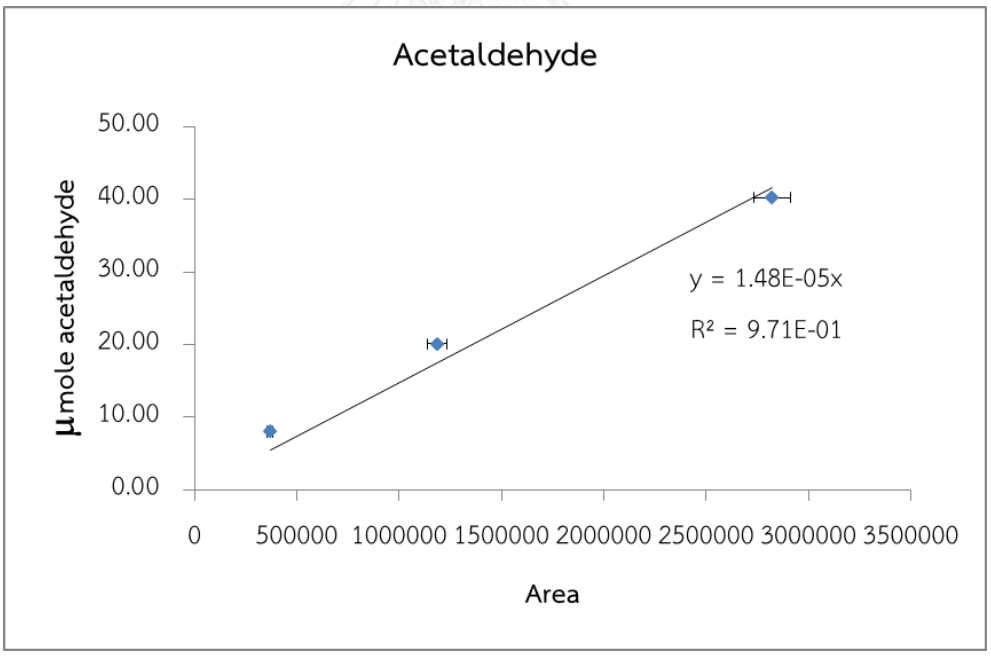

Figure C.4 The calibration curve of acetaldehyde.

APPANDIX D

CONVERSION, SELECTIVITY AND YIELD

The catalytic performance for the ethanol conversion was evaluated in term of activity for ethanol conversion.

C.1 Ethanol conversion

$$\text{Ethanol conversion (\%)} = \frac{(\text{mole of ethanol in feed} - \text{mole of ethanol in product}) \times 100}{\text{mole of ethanol in feed}}$$

Products selectivity are defined as moles of products converted with respect to product in out of reaction as follows:

C.2 Selectivity of product

$$\text{Ethylene selectivity (\%)} = \frac{\text{mole of ethylene in product} \times 100}{\text{mole of total products}}$$

$$\text{Diethyl ether selectivity (\%)} = \frac{\text{mole of DEE in product} \times 100}{\text{mole of total products}}$$

$$\text{Acetaldehyde selectivity (\%)} = \frac{\text{mole of acetaldehyde in product} \times 100}{\text{mole of total products}}$$

Where: Total product is mole of (Ethylene + DEE + Acetaldehyde).

Products yield was evaluated in term of ethanol conversion and products selectivity

$$\text{Ethylene yield (\%)} = \frac{\text{ethylene selectivity} \times \text{ethanol conversion}}{100}$$

$$\text{DEE yield (\%)} = \frac{\text{DEE selectivity} \times \text{ethanol conversion}}{100}$$

$$\text{Acetaldehyde yield (\%)} = \frac{\text{acetaldehyde selectivity} \times \text{ethanol conversion}}{100}$$

From calibration curve;

Mole of ethanol = (2.31×10^{-5}) x area

Mole of ethylene = (1.03×10^{-5}) x area

Mole of diethylether = (9.06×10^{-6}) x area

Mole of acetaldehyde = (1.48×10^{-5}) x area

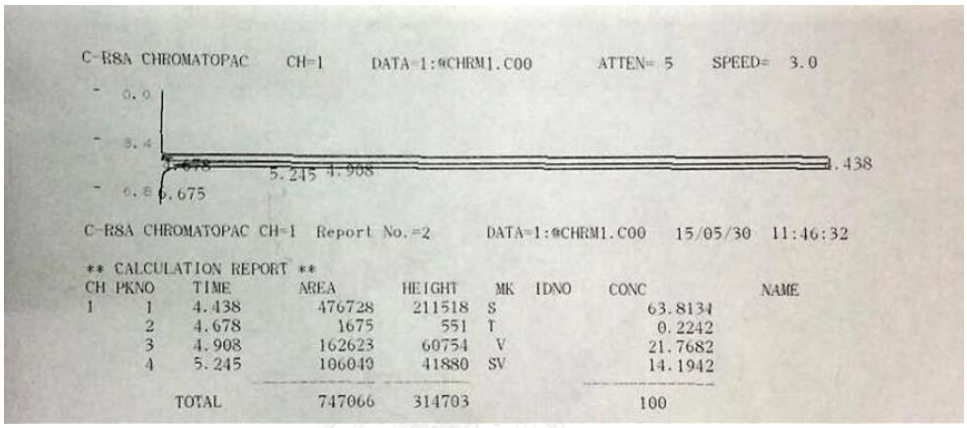

Figure D.1 The GC result

Example;

From **Figure D.1**, the area of reactant and product can be detected by gas chromatography. The peak at 4.438 minute shown area of ethylene, while peak at 4.678, 4.908 and 5.245 minute represented area of acetaldehyde, ethanol and diethylether, respectively.

So, mole of ethanol = (2.31×10^{-5}) x 162623

= 3.76 mole

APPANDIX E

LIST OF PUBLICATION

Journal

Tanutporn Kamsuwan and Bunjerd jongsomjit “A comparative study of different Al-based solid acid catalysts for catalytic dehydration of ethanol.” Journal of the ENGINEERING JOURNAL

Proceeding

Tanutporn Kamsuwan and Bunjerd jongsomjit, “Characteristics, catalytic properties and stability of Al-based solid acid catalysts for ethanol dehydration reaction.” Proceeding of the PACCON 2016, BITEC Bangkok, Thailand, January 9-11, 2016.

VITA

Miss Tanutporn Kamsuwan was born on July 30, 1990 in Uttaradit, Thailand. She graduated the Bachelor's Degree of Engineering from the Department of Chemical Engineering, Faculty of Engineering and Industrial Technology, Silpakorn University (SU) in October 2013. She continued the Master of Engineering in Chemical Engineering, Chulalongkorn University (CU) in August 2014.